UNIVERSITA' DEGLI STUDI DI PADOVA

DIPARTIMENTO DI SALUTE DELLA DONNA E DEL BAMBINO

CORSO DI DOTTORATO IN MEDICINA DELLO SVILUPPO E SCIENZE DELLA PROGRAMMAZIONE SANITARIA

Curriculum: Emato-oncologia, Genetica, Malattie rare e Medicina predittiva

ciclo 33°

"Study of extracellular matrix in healthy and pathological condition"

Tesi redatta con il contributo finanziario di
Istituto di Ricerca Città della Speranza

Coordinatore: Ch.mo Prof. **Carlo Giaquinto**
Supervisore: Ch.mo Prof. **Piergiorgio Gamba**
Co-Supervisore: Dott.ssa. **Martina Piccoli**

Dottorando: **Edoardo Maghin**

Contents

Riassunto

Introduzione

Il muscolo scheletrico è il tessuto più abbondane del corpo, e grazie alla sua funzione contrattile ci permette di eseguire movimenti volontari e involontari essenziali. È formato da fibre muscolari multinucleate raggruppate in fascicoli; le fibre muscolari risiedono in un'impalcatura tridimensionale, chiamata matrice extracellulare (ECM), composta da una complessa rete di diversi tipi di collageni, glicoproteine, proteoglicani ed elastina, prodotti prevalentemente dai fibroblasti residenti. Per decenni, l'ECM è stata considerata un componente del tessuto relativamente inerte, ma la ricerca attuale rivela che essa regola l'embriogenesi muscolare, la distribuzione spaziale e la crescita delle fibre muscolari, l'omeostasi e la riparazione del tessuto, ed è anche essenziale per un'efficace contrazione muscolare, per la trasmissione della forza e la funzionalità del tessuto. Diverse malattie umane sono associate a disfunzioni e disregolazioni del turnover delle proteine dell'ECM e diversi componenti sono coinvolti in patologie che colpiscono quasi tutti i tessuti del corpo. Ad esempio, nelle sarcoglicanopatie, l'assenza di un componente chiave del complesso distroglicanico, struttura che fornisce stabilità alle membrane muscolari, comporta un'elevata suscettibilità delle fibre muscolari agli stress meccanici. Esistono anche altre tipologie di danni muscolari: una comune malformazione neonatale, l'ernia diaframmatica congenita (CDH), evidenzia la funzione critica del muscolo diaframmatico. L'ernia si sviluppa quando il diaframma non riesce a formarsi e chiudersi completamente, lasciando un "buco" che consente al contenuto addominale di risalire nella cavità toracica ed impedendo così lo sviluppo corretto di cuore e polmoni. Per i difetti di grandi dimensioni, il trattamento chirurgico attuale è l'uso di cerotti protesici per chiudere la malformazione, ma questi materiali non si integrano e non crescono con il bambino, portando a frequenti recidive e comorbilità. Come soluzioni alternative vengono utilizzati diversi scaffold biologici; tuttavia, i risultati complessivi sono paragonabili ad altri materiali protesici più comuni e accessibili. Recentemente abbiamo caratterizzato l'ECM decellularizata (dECM) ottenuta da diaframma di topo sano. La dECM possiede caratteristiche strutturali, biochimiche e biomeccaniche simili a quelle del tessuto nativo. Abbiamo mostrato per la prima volta la superiorità della dECM del diaframma per la chiusura di un difetto diaframmatico in un nuovo modello murino chirurgico di ernia diaframmatica ed anche la produzione in vitro di un costrutto ingegnerizzato vitale e

funzionale che combina dECM sana e precursori miogenici umani in condizione di cultura statica.

Scopo

1. Caratterizzare e confrontare la dECM ottenuta da topi sani e topi αSG KO malati;
2. messa a punto di un bioreattore dinamico, specificamente progettato per la ricellularizzazione di matrici diaframmatiche, al fine di stimolare fisiologicamente le cellule umane (progenitori miogenici e fibroblasti) e ricellularizzare in modo appropriato la matrice, aumentandone l'attecchimento, la disposizione, l'orientamento e la maturità;
3. analizzare il crosstalk tra cellule umane e dECM d'origine sana e patologica;
4. set-up di un protocollo di decellularizzazione del diaframma di maiale, al fine di produrre un biomateriale compatibile e clinicamente rilevante come soluzione alternativa e biocompatibile per il trattamento di grandi difetti dell'ernia diaframmatica congenita.

Materiali e metodi

Abbiamo confrontato e caratterizzato la dECM da tessuto sano e patologico. Abbiamo progettato e sviluppato un bioreattore dinamico mediante modellazione FEM, specifico per il muscolo diaframmatico, e abbiamo stabilito procedure di ricellularizzazione e protocolli di stimolazione dinamica per produrre un modello 3D personalizzato diaframmatico in vitro. Inoltre abbiamo valutato diverse strategie di decellularizzazione (perfusione e diffusione), protocolli di lavoro e step di sterilizzazione al fine di produrre una dECM clinicamente rilevante ottenuta da diaframmi di maialini.

Risultati e discussione

Abbiamo sviluppato il sistema bioreattore che sfrutta la pressione idraulica per stimolare meccanicamente il costrutto diaframmatico in direzione radiale, con controllo dei parametri di deformazione programmabile e singolarmente regolabile. Abbiamo eseguito in parallelo esperimenti statici e dinamici e valutato le differenze in termini di distribuzione cellulare, differenziazione e maturazione, dimostrando l'importanza di una stimolazione meccanica specifica per ottenere costrutti diaframmatici 3D più performanti. L'effetto della coltura dinamica e dell'applicazione di stimoli meccanici è stata evidente sin dall'inizio, influenzando la distribuzione cellulare all'interno del costrutto nonostante una quantità di cellule uguale rispetto

alla coltura statica. Siamo stati anche in grado di caratterizzare e produrre costrutti patologici simili a diaframmi, dove osserviamo, a differenza dei costrutti sani, che la dECM da αSG KO ha arrestato o almeno ridotto la diffusione cellulare che risulta molto simile tra campioni statici e dinamici, eliminando in qualche modo l'effetto positivo ottenuto con la stimolazione meccanica. Infine, abbiamo traslato il nostro approccio e il nostro metodo di decellularizzazione per ottenere delle dECM clinicamente rilevanti da donatori suini. Abbiamo analizzato ed applicato alcuni parametri clinici, come le procedure di sterilizzazione terminale, che devono essere rispettati per tradurre i nostri risultati nella pratica clinica.

Conclusioni

In conclusione, i nostri risultati dimostrano che è possibile adottare un approccio di ingegneria tissutale per proporre nuovi modelli di studio delle patogenesi muscolari ma anche come soluzione alternative alle odierne tecniche di trattamento della CDH.

Abstract

Introduction

Skeletal muscle is a contractile tissue that powers all movement of the body; It is formed by multinucleated muscle fibers that are grouped in fascicles. Muscle fibers reside in a three-dimensional scaffolding, call extracellular matrix (ECM), composed by a complex meshwork of different types of collagens, glycoproteins, proteoglycans, and elastin that are produced predominantly by resident fibroblast. For decades, the ECM was considered a relatively inert tissue component, but current research reveals that regulates muscle embryogenesis, spatial distribution and growth of muscle fibers, homeostasis and repair, and it is also essential for effective muscle contraction, force transmission and functionality. Several human diseases are coupled with dysfunctions and dysregulation of ECM turnover, and several ECM components are involved in pathologies that affect almost all body's tissue. For instance, in sarcoglycanopathies, the absence of a key component of the DGC provide muscle cells susceptible to stretch-induced damage and fiber necrosis, even if the complete sequence of events is not fully disclosed. In humans, a common neonatal malformation, the congenital diaphragmatic hernia (CDH), highlights the diaphragm's critical function. CDH occurs when diaphragm fails to fully form and close properly, leaving a defect that allows abdominal contents herniation into the thoracic cavity that impede lung and hearth development. For large CDH defects, the current treatment is the use of prosthetic patches to close the malformation, but these materials do not evolve with the child growth, leading to frequent recurrences and co-morbidities. Different biologic scaffolds are used for the treatment of CDH; however, overall results are comparable to other more common and accessible prosthetic materials. Recently we characterized the decellularized diaphragm ECM (dECM) obtained from healthy mouse diaphragm. dECM possesses structural, biochemical and biomechanical characteristics similar to those of the native tissue. We showed for the first time the superiority of decellularized diaphragm dECM for the closure of a diaphragmatic defect in a new surgical murine model of diaphragmatic hernia in vivo and also the production in vitro of a viable and functional engineered construct combining healthy dECM and human myogenic progenitors in static culture condition.

Aim

1. Characterize and compare decellularized ECM from healthy and αSG KO mice;
2. Set-up of a dynamic bioreactor culture, specifically design for diaphragm-like muscle tissue construct, in order to physiological stimulate human cells (myogenic progenitors and fibroblast) to recellularized in the proper manner the dECM, boosting cells engraftment, disposition and orientation, and finally maturation;
3. Analyze the crosstalk between human cells and healthy and pathological derived diaphragmatic dECM;
4. Set-up and optimization strategy to produce a clinically relevant dECM patch derived from porcine native diaphragm, to propose a new biocompatible solution for the treatment of large CDH defect.

Materials and methods

We compare and characterized healthy and pathological derived dECM. We design and set-up a dynamic bioreactor culture by means of FEM modelling, specifically developed for engineered diaphragm-like construct, and we established a recellularization procedures and dynamic stimulation protocol to produce advance 3D tissue model in vitro. We evaluate different decellularization strategy (perfusion vs diffusion), methods and step in order to produce clinically relevant dECM patch from porcine diaphragm source.

Results and discussion

We developed the bioreactor system that exploits hydraulic pressure to mechanically strain the diaphragm-like construct in a radial direction, with programmable and individually tunable control of strain parameters. We performed in parallel static and dynamic experiments and evaluated the differences in terms of cell distribution, differentiation and maturation, demonstrating the importance of specific mechanical stimulation to obtain more performing 3D diaphragmatic constructs. The effect of dynamic culture and application of mechanical stimulus was evident far from the beginning, influencing transversal cell distribution inside the construct despite an equal cell amount compared to static culture. We also were able to characterized and produce pathological diaphragm-like construct, where we observe, differently from healthy scaffolds, αSG KO dECM arrested or at least reduced cell spreading that resulted very similar between static and dynamic samples, abolishing in some way the positive effect obtained with

mechanical stimulation. We translated our approach and decellularization method to obtain a relevant dECM from porcine source, investigating the clinical needs and parameters, such as terminal sterilization procedures, that requires to be achieved to finally translate our results into the clinical practice.

Conclusions

Taken together these results demonstrate the possibility to adopt our multi-step tissue engineered approach to propose new models and solution for the treatments of CDH.

1. Introduction

1.1.1 Skeletal muscle and extracellular matrix

Skeletal muscle is a contractile tissue that powers all movement of the body; is the most abundant and distributed tissue with specific and distinct functions, typically accounting for more than 30% - 40% of total body mass. It is formed by post mitotic cylindrical multinucleated cells (less than 100 μm in diameter), called muscle fibers that are grouped in fascicles. Muscle fibers reside in a three-dimensional scaffolding composed by a complex meshwork of different types of collagens, glycoproteins, proteoglycans, and elastin, and is commonly referred to as extracellular matrix (ECM)[1, 2] Muscle fibers derive from the fusion of undifferentiated cells, known as myoblast or muscle precursor cells (MPCs). The contractile unit in the skeletal muscle is the sarcomere, in which myosin and actin, the cytoplasmic proteins responsible for muscle contraction, are arranged in myofibrils, the basic functional unit of the muscles, which run parallels along the muscle axis (the repetitive distribution of myofibrils confers to the skeletal muscle its typical banding pattern). Each mature muscle fiber is innervated by a branch of motoneurons and surrounded by vessels [1]. Skeletal muscle cellular components are mediators and targets of multiple signals provided by both external and internal stimuli, such as growth factors entrapped into the ECM. They act as dynamic players that can change their behaviors in response to these cues. For decades, the main focus in the study of muscle regeneration was the muscle stem cell compartment; however, the multiple specific interaction of stem cells with stromal cells and ECM and the crucial role of these relationships in tissue homeostasis and regeneration, are now emerging. In mature tissue, muscle regeneration relies on adult resident stem cells, called satellite cells (SCs) [2]. They are normally in a quiescent state, homing in an anatomically microenvironment defined as the stem cell niche, which is juxtaposed between the sarcolemma and the specialized basal lamina that surrounds the muscle fibers. The SC niche acts as an instructive environment, where communication between ECM and SCs is critical in the balance between quiescence and activation phase, and in maintaining the stem cell pool. SCs interact with microenvironment via physical and biochemical stimuli. They are able to bind ECM molecules such as collagen VI and fibronectin through integrin receptors, and also to detect secreted paracrine factors by surrounding cells and ECM [3].

Mild injury induces muscle fibers break and recruitment of surrounding SCs on the intact part of the fibers. In contrast, severe injury triggers complete myofibers destruction followed by SCs proliferation and differentiation on ECM debris referred to as “ghost fibers”. These injuries activate a tightly controlled myogenic process, regulated by key transcription factors. During homeostasis, SCs are quiescent and express Pax7 and Myf5, and Notch signalling is highly active. When activated upon trauma, they rapidly upregulate Myod and Myf5, and Pax7 protein remains detectable. Following the amplification phase, myoblasts express the terminal differentiation gene Myogenin and exit the cell cycle [4]. Differentiated myoblasts fuse to the pre-existing fibers (mild injury) or together (severe injury) to form new fibers. During the first phases of this process, some SCs self-renew to replenish the stem cell pool and guarantee a long-lasting regeneration potential [5, 6]. Fibroblasts, which reside in the interstitial space between muscle fibers, secrete the majority of the skeletal muscle ECM, including structural proteins such as collagen I, III, IV, VI, fibronectin, but also metalloproteases, and proteoglycans. These cells are responsible for muscle structure healthiness maintenance during tissue homeostasis, providing mechanical stability, integrity and functionality to the muscle fibers. Fibroblasts and SCs reciprocally cross-talk during muscle regeneration, with fibroblasts acting as a component regulating the niche and as paracrine growth factor source, positively regulating SCs expansion and differentiation timing, and ensuring an efficient and complete muscle regeneration [7].

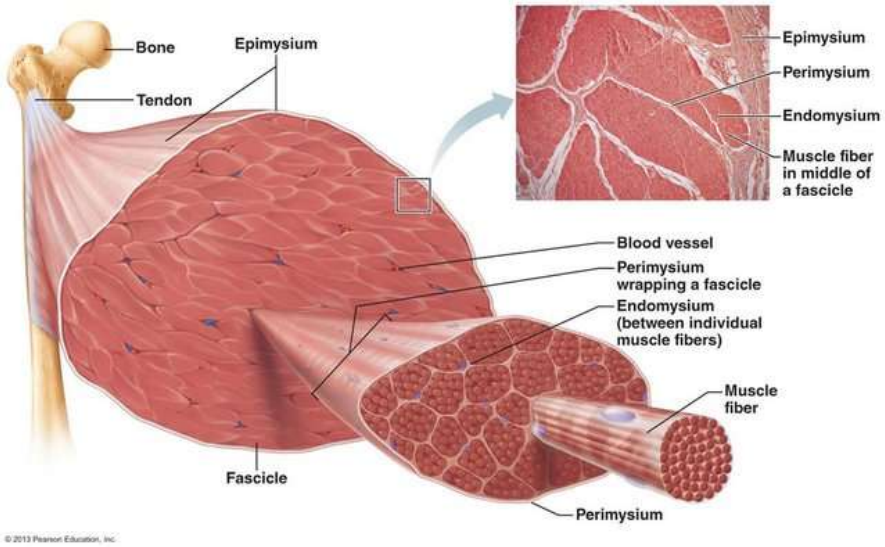

Fig. 1.1 Skeletal muscle tissue anatomy and organization

(Source: https://quizlet.com/237782737/chapter-9-figure-91-connective-tissue-sheaths-of-skeletal-muscle epimysium-perimysium-and-endomysium-diagram/)

1.1.2 ECM composition and structure

For decades, the ECM was considered a relatively inert tissue component, but current research reveals the involvement of ECM in a large important physiological process. ECM regulates muscle development, spatial distribution and growth of muscle fibers, homeostasis and repair, and it is also essential for effective muscle contraction, force transmission and ultimately ensures a proper functionality. The muscle ECM is comprised of various fibrous proteins (e.g., collagens) and proteoglycans, produced predominantly by resident fibroblast [8, 9]. The muscle ECM has two principal types of conformation: 1) interstitial matrix (epimysium and perimysium), a connective tissue matrix formed by a mixtures of collagens, elastin, fibronectin, proteoglycans, and glycosaminoglycans, and 2) pericellular matrix (basement membrane), which interact with cells and has different and specific molecular composition (e.g. basal lamina) [10]. Anatomically (Fig. 1.1), muscle ECM is organized in three layers: the endomysium envelops individual myofibers, the perimysium bundles myofibers into fascicles, and the epimysium surrounds anatomical muscles and links to the tendons at the myotendinous junctions. Collagen is the main structural protein in muscle ECM (1 to 10% of dry weight) [11] and it is composed by three polypeptide α-chains that form a triple stranded helix, which can assemble into macromolecule complexes, such as fibrils and networks. Although a total of 28 different collagen molecules can coexist in a heterogeneous mix, generally a single or few type of collagen predominate in a tissue-specific manner, like collagen types I and III in skeletal muscle. Collagen I has been reported to be the predominant perimysium collagen, while collagen III is distributed between endomysium and epimysium [12]. Fibronectin is another fibrous protein that plays an important role in cell adhesion and migration. Fibronectin binds the integrin adhesion receptors on cell surface, and it has been shown to be able to bind several growth factors, acting as reservoir for different molecules and growth factors. Another class of cross-linked glycoproteins is represented by laminins, which are mainly localized in the basement membrane. They exist in many forms, depending on the different composition of chain peptides (e.g. α1, β1, and γ1). Laminins turnover during muscle embryogenesis, adult homeostasis and tissue regeneration are fundamental to control the precise and specific SCs activation, expansion and self-renewal. The endomysium directly interacts with the myofiber sarcolemma at the specialized basal lamina, which consists primarily of type IV collagen and laminin α2 in the adult mature muscle. Laminin, in turn, serves as ligand for two sarcolemma receptors – the dystrophin-associated glycoprotein

complex (DGC) and the α7β1 integrin [15, 16]. Integrins act in a bidirectional manner, converting the extracellular signals to intracellular response, allowing cells to sense their surrounding microenvironment and actively modulating their processes and behavior. Specifically, integrins link the actin microfilaments of the cytoskeleton with ECM, working also as a sensor of tensile strain. The DGC is a fundamental player in providing a mechanical linkage between the contractile components of skeletal muscle and the interconnected layers of the muscle ECM, stabilizing the sarcolemma (Fig. 1.2). The principal protein of the DGC complex is Dystrophin, a cytoskeletal protein that is involved in attaching F-actin to the muscle ECM. It is encoded by the DMD gene, one of the longest human genes known, covering 2.3 megabases [13]. ECM is subjected to regular cycles of alterations, degradation, as well as reassembly. Scientific evidence further demonstrates that, in addition to this structural role, the interaction between myoblasts, differentiated muscle fibers and ECM components is of central importance for the embryonal development, further growth, and repair of muscle tissue.

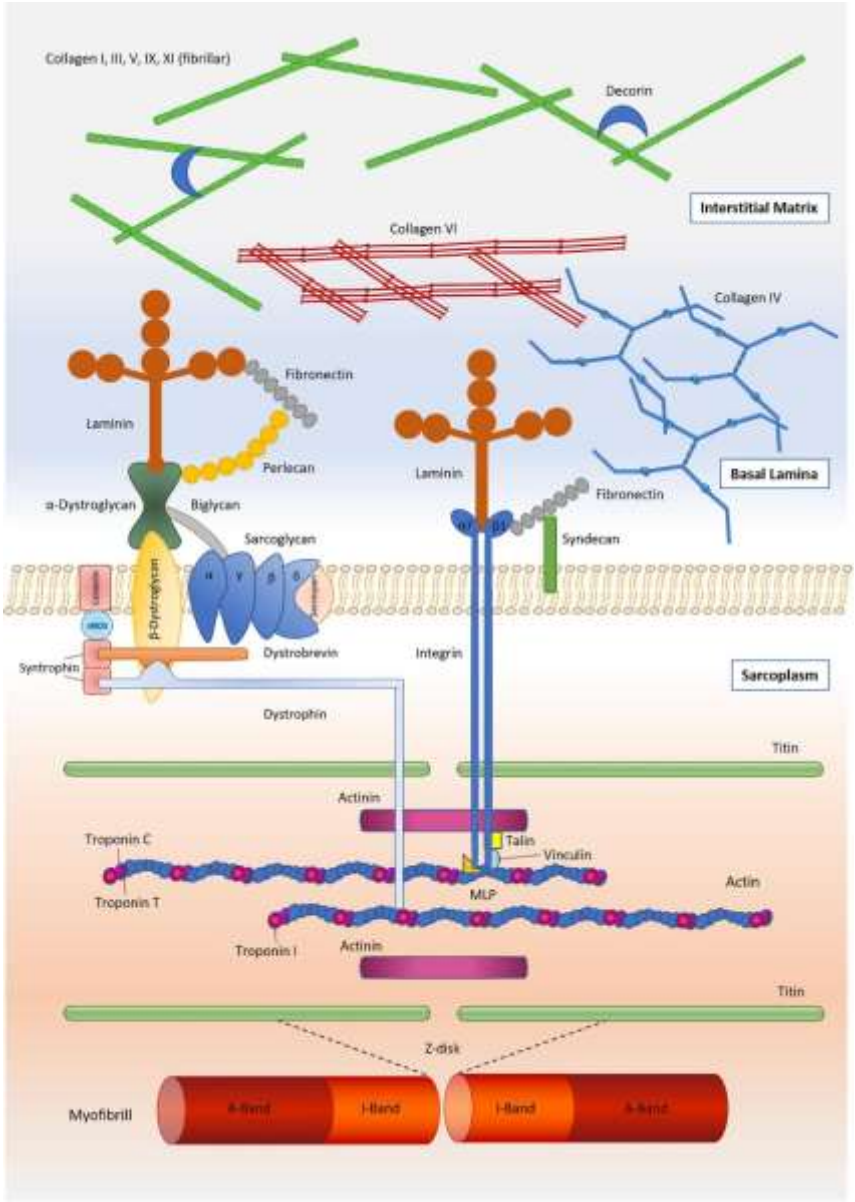

Fig.1.2 Skeletal muscle Extracellular Matrix

(Source: Caspo et al. Front. Physiol., 19 March 2020 | https://doi.org/10.3389/fphys.2020.00253)

1.1.3 Skeletal muscle and ECM during embryogenesis and development

The cellular source of muscle ECM are fibroblasts, which originate from different embryonal sources, including the somites, the lateral plate mesoderm and the neural crest. Muscle development occurs via two interconnected processes, myogenesis (formation of muscle progenitors and their differentiation into multinucleate myofibers) and muscle morphogenesis (the process by which myofibers are assembled into well arrange and organized muscles) [14,

15]. Recent research has provided new insight on muscle fibroblasts and the connective tissue they produce it seems that it influences both myogenesis and muscle morphogenesis, thus acting as important regulator of muscle development. Myogenesis is a well-defined pathway that is similar among all body muscles, whereas muscle morphogenesis occurs in a unique and specific manner for anatomically different muscles that have to be arranged into a stereotyped spatial array. Morphogenesis involves the migration of muscle progenitors to specific regions, the regulation of myoblast number, the selective differentiation of muscle progenitors into myofibers, the spatial distribution, the elongation and the increase in size of myofibers via selective myoblast fusion. Finally, it regulates the integration of myofibers with muscle ECM, vessels, nerves, tendons, and bones. The diaphragmatic muscle for instance, is a unique mammalian muscle that exert the main breathing function and it is peculiar for anatomical arrangement and formation. During development, the diaphragm muscle and ECM originate from two different embryonic sources. Similar to axial and limb muscles, the diaphragm's MPCs arises from the somites and recently was shown to specifically come from cervical level somites. The diaphragm's fibroblasts that secret the ECM comes from the pleuroperitoneal folds (PPFs), a lateral plate-derived pyramidal tissue located between the thoracic (pleural) and abdominal (peritoneal) cavities. MPCs migrate from the cervical somites to the PPFs, and as the PPFs spread the MPCs are carried throughout the growing diaphragm and differentiate into the radially oriented myofibers of the costal diaphragm in close association with the muscle ECM. Multiple studies demonstrate that the PPFs, and likely the PPF-derived ECM, control diaphragm development. The normal morphogenetic expansion of the PPFs ahead of muscle, nerve and vasculature elements suggested that the PPFs regulate the morphogenesis of the diaphragmatic muscle [16]. Defects in muscle ECM development or its communication with neighboring muscle have also emerged as a source of congenital birth defects in head and limb muscles and in the diaphragm.What precisely is the molecular communication between the ECM fibroblasts and MPCs remains an open question [17].

1.1.4 Skeletal muscle and ECM crosstalk during homeostasis, regeneration and repair

Functionally, the ECM serves as network for the transmission of contractile force, which increases the efficiency of muscular contraction but also protects the muscle fibers from

excessive stress and facilitates healing of microtrauma. In addition to its structural role, the ECM is actively involved in the regulation of the muscle's pool of SCs. ECM can also bind and store several soluble growth factors, which are released during ECM remodeling and degradation in physiological homeostasis or repair, creating a gradient of signaling molecules that are free to bind to the relative cell receptor and influence cell behaviors [18].

ECM niche physically protects SCs from entering the cell cycle, acting as a mechanical barrier and thus, helps to maintain the muscle's regenerative potential. After trauma and consequent activation, SCs actively modify the ECM within their niche by releasing enzymes that catalyze the remodeling of the SC basal lamina and by synthesizing sequentially laminin-α1 and laminin-α5, two laminin subunits that are normally specifically produced during embryonic myogenesis. Indeed, laminin-111 secreted during this process is essential for SC expansion and self-renewal, a process mediated by the signaling of laminin-α1 through integrin-α6 receptor. While laminin-111 is associates directly with SCs via its receptors, both collagen VI and fibronectin are mostly present into fibrillar networks, components of the interstitial matrix associated with fibroblasts. Collagen VI and fibronectin are involved in the control of SC activity and self-renewal, suggesting that remodeling of the ECM following muscle injury and SC activation is a widespread mechanism to maintain a stem cell pool [23, 24].

1.1.5 Pathological skeletal muscle ECM

Several human diseases are coupled with dysfunctions and dysregulation of ECM turnover, and several ECM components are involved in pathologies that affect almost all body's tissue. These ECM-linked diseases are generally attributable to factors ranging from abnormal signaling functions to instability of structural components [19]. Different skeletal muscles associated genetic disorders are typically caused by mutations in ECM genes that encode ECM proteins and their transmembrane cell receptors that can result in diverse skeletal muscle diseases, a large proportion of which are types of fibrosis and muscular dystrophy [20].

Collagen Myopathy

Collagens are reported to be present in almost all the connective tissue of the body, they fulfill a number of critical functions in skeletal muscle including the transmission of forces to bones, tensile strength, and elasticity, and are also involved in the regulations of cell attachment and

differentiation. Collagens also play critical roles in cell-to-ECM interactions via several and specific transmembrane receptors. Collagen VI is a specific component of muscle ECM endomysium and allows muscle cells to connect with the ECM by interacting with perlecan in the basal lamina [21]. It is formed by three polypeptide chains (a1, a2, a3), which are encoded by COL6A1, COL6A2 and by COL6A3 genes [22]. Mutations in all three of these genes result in two main muscle disorders, namely; 1) Ullrich congenital muscular dystrophy (UCMD) (severe phenotype) and 2) Bethlem myopathy (minor to moderate phenotype). Recently, two additional phenotypes were found to be associated with mutations in the COL6A2 gene: a limb-girdle muscular dystrophy and myosclerosis [23].

Muscular dystrophy

Muscular dystrophy is a collection of genetic diseases characterized by skeletal muscle weakness and progressive degeneration over time of muscle fibers that are replaced by fibrosis and fat, making muscle tissues less able to generate force. Respiratory failure, resulting from the weakening of the diaphragm, may limit lifespan in muscular dystrophy patients unless mechanical support is instituted [24]. Different loss of function mutations in the genes encoding dystrophin, or the associated proteins in the DGC, triggers instability of the sarcolemma and consequent and progressive myofiber loss. Mutations in dystrophin have been extensively studied and cataloged providing remarkable structure-function correlation between predicted protein structure and complex clinical outcomes. Multiple smaller isoforms of dystrophin sharing the same C-terminal extremity are transcribed from several intronic promoters within the dystrophin gene. Duchenne (DMD) and Becker (BMD) muscular dystrophies are the most know and common types. Generally, DMD patients exhibit an absence of dystrophin while BMD patients often harbor internally deleted but partially functional dystrophin proteins. In DMD patients and in the mdx mouse model of dystrophin deficiency, loss of dystrophin results in a major reduction of the entire DGC complex, and thereby the linkage between muscle fiber cytoskeleton and the ECM, thus the destabilized sarcolemma becomes fragile and less resistant to mechanical stress, which in turn leads to fiber damaged and loss with membrane leakage, altered calcium homeostasis, subsequent cell death and ultimately tissue dysfunction [25].

Sarcoglycanopathies

Sarcoglycanopathies are included in a large group of heterogeneous limb-girdle muscular dystrophy, due to an autosomal recessive muscle-wasting disorders caused by genetic defects in one of four cell membrane glycoproteins, a-, b-, g- or d-sarcoglycan. These four sarcoglycans form tetrameric subcomplex that is closely linked to the DGC complex, serving as anchorage for the peripheral components. These transmembrane proteins display a short intracellular tail, and a large extracellular glycosylated domain rich in cysteine residues, ranging from 50 to 35 kDa. Specifically, one type, Limb-girdle muscular dystrophy type 2D (LGMD2D) is caused by mutations in the SGCA gene coding for α-sarcoglycan (αSG). Sarcoglycan complex, as part of DGC, plays a key role in maintaining the sarcolemma stability and integrity during muscle contraction, and seems involved in signaling processes [26]. Their biosynthesis occurs into the endoplasmic reticulum (ER) where they undergo folding, glycosylation and assembly into the tetrameric complex that eventually moves toward the sarcolemma. In sarcoglycanopathies, a strong reduction/loss of the mutated protein as well as of the wild type partners occurs, irrespectively of the SGC gene involved and of the type of mutation present; many different genetic defects have been described, with missense mutations being the most frequently reported. In sarcoglycanopathies, like in DMD, the absence of a key component of the DGC provide muscle cells susceptible to stretch-induced damage and fiber necrosis, even if the complete sequence of events is not fully disclosed [27].

1.2.1 Tissue Engineering approaches for congenital diaphragmatic hernia

Diaphragm, as before mentioned, is a unique mammalian muscle due to its anatomical conformation and function. It is a domed muscle lying at the base of the thoracic cavity that is essential for breathing and for separating the abdominal organs from the thoracic cavity containing the heart and lungs (Fig. 1.5). In humans, a common neonatal malformation, the congenital diaphragmatic hernia (CDH), highlights the diaphragm's critical function. CDH occurs when diaphragm fails to fully form and close properly during embryonic development, leaving a defect that allows abdominal contents herniation into the thoracic cavity that impede

lung and hearth development. CDH occurs in approximately 1 in 2500-3500 births, has an overall survival rate of 50% and long-term morbidity [28]. Despite the identification of many CDH-associated genes, the etiology is not yet complete understood. PPF-derived ECM fibroblasts guide normal diaphragm muscle development and defects in ECM development or in the crosstalk communication between fibroblast and muscle cells lead to CDH. Nowadays, 80% of CDH cases are prenatally diagnosed and the current clinical standard solutions are respiratory problem treatment and the closure of muscle defect. Lung development could already be stimulated prenatally by foetal endoscopic tracheal occlusion (FETO) but ultimately the surgical repair operation is often required, with 60-70% of patients that present small defect that required only primary closure of the native diaphragm [29]. For large CDH defects, the current treatment is the use of prosthetic patches to close the malformation, but these materials do not evolve with the child growth, leading to frequent recurrences and co-morbidities. Nowadays, Gore-Tex® is the most frequently used non-absorbable synthetic patch [30, 31]. However, the application of Gore-Tex® is often associated with several complications such as adhesion, breathing abnormality, thoracic and spinal column deformities and hernia recurrence in around 50% of patients. This is due to the different biomechanical properties of Gore-Tex® compared to the native diaphragm and lack of grow with the child. When hernia reoccurs, children have to undergo multiple surgeries, increasing the risk of infections and drawbacks [32, 33]. As alternative biological-derived patch, several non-tissue specific acellular matrices were used to treat CDH (Alloderm®, Pericardial tissue, SurgAssist®) and, despite their biocompatibility and efficiency when used in other organs, the overall results in terms of drawbacks and hernia recurrences were poorer than those of standard Gore-Tex patch treatment [34, 35]. The therapeutic potential of tissue specific decellularized scaffolds to promote skeletal muscle regeneration has been supported by different studies and data and given the current suboptimal repair methods as to be validate and optimized for the treatment of CDH [36-38].

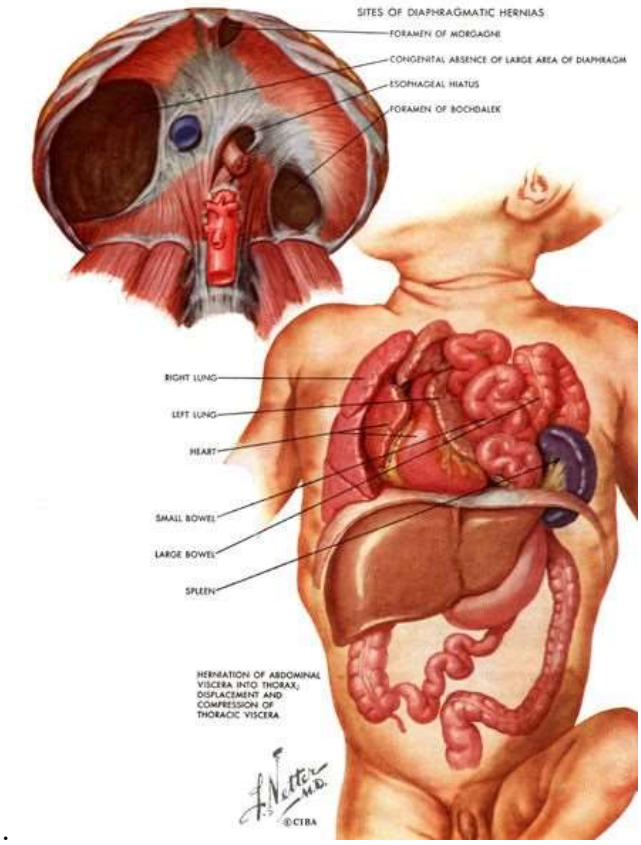

Fig. 1.5 Congenital Diaphragmatic Hernia

(Source: http://courses.md.huji.ac.il/96854_e/Congenital_diaphragmatic_hernia/slide_17.htm)

1.2.2 Decellularized ECM

Different tissue engineering approaches are found in literature to generate in vitro 3D muscle constructs, and recellularization of decellularized scaffolds has given important results on the study of cellular behavior when grown in a 3D context, and as a possible clinical approach for the treatment of major muscle malformations, injuries and congenital defects. Naturally derived biomaterials have proven to be superior to synthetic polymers as regenerative medicine matrix scaffolds, in that they can retain the hierarchical complexity of native tissues [48]. Decellularized ECM (dECM) derived from organs/tissues encompass the characteristics of an ideal tissue scaffold: complex composition, vascular networks, and unique tissue-specific architecture and composition. Consequently, their use has propagated throughout regenerative medicine both in vitro and in vivo [39, 40].

By using biologic matrices as scaffold that recapitulate native tissue to varying degrees, it is possible to augment the biocompatibility within the host tissue and increase cell retention and survival, enhancing the effectiveness of cell-based repair. ECM can be used to deliver or retain cells in vivo, but it can also serve as cell support to engineer complex 3D tissues in vitro. Finally, dECM scaffolds can be used stand-alone to facilitate delivery of other biologics such as small molecules, growth factors or genes that either obviate the need for cells or provide new exciting natural niches for host cell recruitment. Decellularized ECM derived from native tissues in which the cellular component is removed whereas, structural and functional ECM proteins are preserved. There are various accepted methods for tissue decellularization; however, no method is recognized as optimal due to variability in tissue composition, structure and complexity. Physical methods of decellularization include multiple freeze-thaw cycles to disrupt the cellular components, agitation during immersion in chemical solution, and application of pressure or supercritical fluids. Although these methods have proven effective in some tissues, they can also damage the ECM ultrastructure and mechanical properties [41]. Enzymatic decellularization cleaves cell membranes, cell-cell attachments, cell-ECM attachments, or nucleic acid-ECM attachments with specific enzymes such as nucleases, collagenases, and proteases. Chemical decellularization using alkaline and acidic solutions, enzymes, or alcohols can degrade fibrillar matrix components or residual crosslinking of matrix proteins, impacting the strength and stiffness of the matrix [51 – 54].The use of detergents, such as sodium dodecyl sulfate (SDS) or sodium deoxycholate (SDC), Triton-X-100, is suitable for decellularizing whole organs by perfusion through the vasculature or by agitation [42, 43], with minimal ECM disruption if detergent exposure is minimized and optimized. Residual DNA from the decellularization process may be responsible for undesired immune response to dECM, thus some studies suggest that dECM should contain 50 ng dsDNA/mg ECM dry weight [44]. dECM scaffolds have similar tensile strength to native tissues and retain most of the inherent native vasculature, to about the third or fourth level of branching. Perfusion decellularization is a favorable approach for decellularization as it can minimize ECM damage due to excessive mechanical forces while maximizing delivery of decellularizing solutions into deeper parts of the organ. Since dECM scaffolds retain 3D architecture of the native tissue and can provide necessary signaling to modulate cell function, they have been reported to be superior in maintaining and/or guiding stem cell differentiation as compared to plastic tissue culture or natural biomaterials such as collagen [45]. Even powdered or dECM hydrogels supports cell differentiation and survival

better than collagen matrices. The 3D interactions existing among different components of the ECM is far for being a simple overlay of proteins organized in a layer-by-layer fashion [46, 47]. Indeed, ECM components not only interact with each other in specific fashions, but each single component, and also defined isoforms of a same component, are tissue-specific and even site-specific inside a defined tissue [48].

1.2.3 Skeletal muscle decellularized ECM

Severe skeletal muscle injuries resulting from trauma, burns, tumor ablation, congenital or degenerative disease may cause a massive loss of at least 20% of a given skeletal muscle tissue, which is termed volumetric muscle loss (VML) [49]. Even though skeletal muscle has a remarkable capacity to undergo regeneration, several pathological conditions can lead to extensive and irreversible muscle loss: i.e., congenital defects, traumatic injuries, surgical ablations, and neuromuscular diseases. Failure of normal regeneration results in VML, with loss of muscle function, often associated with scar tissue formation and adipose tissue substitution. Current treatments for such conditions have limited success, leading to considerable social and economic burden. Therefore, there is a great need for new regenerative medicine strategies aimed at treating VML conditions [50] [51]. Small intestine submucosa matrix (SIS), urinary bladder matrix (UBM), and skeletal muscle decellularized scaffolds have been the most commonly used materials to repair VML defects. SIS and UBM scaffolds are prepared with standardized protocols, and are commercially available, clinically approved, and have also been used in patients [52]. Conversely, skeletal muscle scaffolds have only been used in animal models, and their preparation has been shown to be a more complex procedure, mainly due to tissue complexity and thickness. The main protocols applied to generate decellularized scaffolds from skeletal muscle are essentially of three types: (A) enzymatic [53-55], (B) detergent [56-58], and (C) detergent-enzymatic treatments (Fig. 1.4) [59, 60].

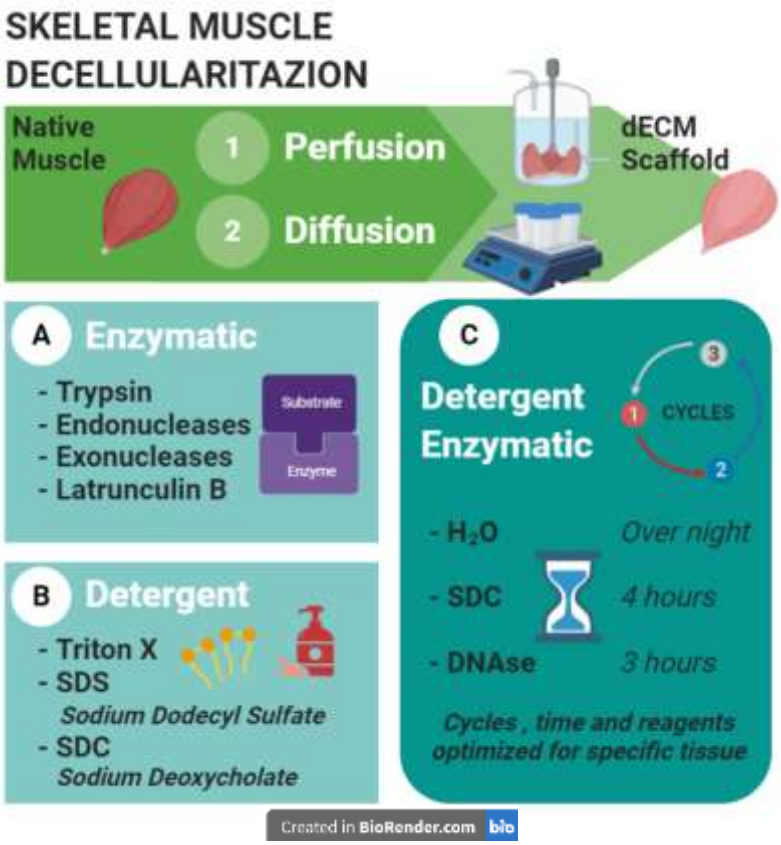

Fig. 1.4 Skeletal Muscle Decellularization methods

In the literature such scaffolds are defined as decellularized; however, some of them would be better defined as "anucleated" rather than "acellular" scaffolds. Indeed, together with the elimination of the nuclear content and the maintenance of the ECM, such treatments can partially preserve cytoplasmic components of the original tissue, in particular those belonging to myofibers [61]. The biological properties retains by the scaffolds depend on the agent used for inducing decellularization, as well as on the method applied (i.e., immersion vs. perfusion) and on the characteristics of the primary tissue/organ (density, cellularity, dominant component in tissue, and thickness) [62]. Another important factor to consider is whether using a tissue-matched decellularized scaffold can have positive effects on regeneration into a specific tissue conformation and environment. SIS and UBM are scaffolds that can fill the volumetric loss of tissue but do not have any muscular specific components. Based on the complexity of the biological meaning of ECM, acellular tissues should be better at instructing host and/or seeded-donor cells toward the regeneration of the tissue of origin [63]. It is important to underline that the large volume of tissue that needs to be regenerated in patients affected by VML can be a

major limiting step for acellular tissue application in clinic. Studies performed on murine and rat VML models have conclusively demonstrated the ability of acellular scaffolds to promote myogenesis both as stand-alone devices and when associated with cell therapy strategies. Interestingly, by comparing the obtained results, it could be speculated that acellular scaffolds derived from skeletal muscle are the best candidate to promote skeletal muscle regeneration in vivo, when compared to SIS and UBM scaffolds [74]. This conclusion seems to be valid not only when scaffolds are used as devices, but also when they are associated with cell therapy. The possibility of using decellularized scaffolds as devices represent an important aspect for their translational application, as it overcomes the limiting steps specifically related to cell therapy [61].

1.2.4 Decellularized ECM and clinical translation

Nowadays, tissue engineering strategies are becoming a clinical reality and relevant progresses are made using decellularized tissue and organs as patch or scaffold to regenerate in vivo tissue substitutes. Decellularization generates specific acellular xenografts that are clinical available; the production of "ready to use" and "off the shelf" biomaterials allow to fill the gap between biomedical research and clinical reality for organ transplantation, opening new opportunities. Nevertheless, these materials must be tested and studied in proper animal models, following standardized guidelines [64]. Several dECM tissues have been FDA and EMA approved as clinical devices in the last decade, including porcine heart valves (Synergraft®), porcine small intestine submucosa (SurgiSIS®) and liver (MIRODERM®). These products have demonstrated clinical safety, efficacy, and retain structural characteristics of ECM, so that they can support cell growth and be remodeled while being relatively non immunogenic [65]. Decellularized ECM that goes into clinic should be treated and regulated as "xenograft" if derived from animal sources and a more comprehensive and specific regulation should be applied to this product to guarantee safety and efficacy. Following the guidelines designated by FDA with "Animal, Product, Preclinical, and Clinical Issues Concerning the Use of Xenotransplantation Products in Humans" document, a key aspect to investigate is the presence or absence within the dECM of Galactose-alpha-1,3-galactose, a well-known xenoantigen that triggers hyperacute and acute rejection (HAR) mechanisms and ultimately causes graft degeneration and failure. However, the dECM key features it is the retention of native complexity and thus the composition of ECM products is more variable than synthetic materials, and the methods of preparation can be very

different from one product to the next. Other important challenges to face include: the often-non-traditional manufacturing methods, the sterilization procedure, the relevance of preclinical models and the fulfillment of appropriate clinical trials [66].

1.2.5 Bioreactor platforms for skeletal muscle modelling

One more key element that needs to be addressed for skeletal muscle tissue engineering is choosing proper stimulation strategies (either mechanical-, electrical-, or electromechanical-stimulation) in order to obtain mature and functional biocompatible substitutes [67]. Over recent years, multiple approaches have been developed to design suitable platforms ensuring the abovementioned stimulation strategies, and in particular, the use of bioreactor systems. Bioreactor is defined as an in vitro culture system that has been designed to mimic the physiological conditions of the tissue of interest, acting on cell behavior, metabolism, and interaction within constructs in order to achieve the proper tissue structure, organization, and ultimately maturation and function [68-70]. In this context, several types of bioreactors have been developed and manufactured to mimic the in vivo tissue environment physiology, providing a powerful and reliable model to study cell-ECM interaction during myogenesis and regeneration [77]. The appropriate bioreactor settings should be developed in relation with the type of biomaterial used for bioscaffold production and taking into account the cues that encapsulated cells require to produce mature tissue. Myogenic cells highly respond to their microenvironment such as the surrounding ECM, mechanical forces, and biochemical signals. Adequate physiochemical and structural properties as well as bioactive cues such as incorporated growth factors to enhance cell adhesion, distribution, and myogenic differentiation, can be added to the bioreactor platform finely mimicking the microenvironment observed in vivo. The application of peculiar stimulation strategies has been pursued by researchers to recapitulate and trigger myocytes alignment, fusion and differentiation. Until now, two main strategies of stimulation have been adopted: the mechanical and electrical stimulations, and their combination [71]. The suitable mechanical environment can be simulated by cyclic and/or static strain, whereas the neural inputs are mimicked by electrical pulses. Kim et al. showed that the relationship between mechanical and electrical stimulations were crucial to obtain in vitro the proper maturation of mature myotubes and organized tissues [72]. Mechanical stimulation represents a fundamental element for myogenic cells and plays a critical role in the regulation of skeletal muscle mass,

cell differentiation, tissue ECM remodeling and homeostasis. In several studies it has been shown that a specific type of stimulation (continuous versus stretched/relaxed stimulation) affected cell distribution, organization but also metabolism, protein synthesis and maturation [80, 83, 85]. The strategy and type of mechanical stimulation applied to the constructs triggered different adaptive response and consequently maturation of the tissue. The main aspect that mechanical stimulation aimed to replicate is the progressive (continuous stimulation) bone elongation, which occurs during muscle embryonic development and is crucial to organize the structure directionality of the tissue, together with the muscle cyclic elongation that occurs during exercise and homeostasis in adulthood (cyclic stimulation). For instance, bone growth elongation can be simulated using a ramp of continuous stretching that is essential to define myotube organization, whereas cyclic stimulation is crucial for the regulation of metabolic activity and growth, regulating glucose uptake and lactate efflux. Moon et al. indeed showed the importance of bioreactor preconditioning in vitro to accelerate skeletal muscle tissue organization, maturation, and contractility of an engineered construct before in vivo application. They observed enhanced functionality of the tissue engineered construct after one week of bioreactor preconditioning culture (using cyclic stimulation) [73]. The application of combined stretch protocols has produced controversial outcomes with both promising beneficial and negative effects. The different observations are likely due to the amount of stretch, frequency and loading protocols applied during the culture into a specific bioreactor setting [77]. Nevertheless, combined ramp and cyclic stretching protocols are essential to fully replicate the transition from an embryonic to a mature mechanical environment in which the muscle is continuously stimulated. Moreover, mechanical stimulation enhances the cross-striations of myotubes and a switch of myosin heavy chain (MYHC) isoforms from embryonic to adult. An appropriate mechanical load protocol can modulate and exert positive effects on gene regulation and protein expression, for both proliferation and differentiation of engrafted cells [74, 75].

1.3.1 Tissue engineering approaches for skeletal muscle modelling, drug discovery and advance personalized treatment

The loss or failure of organs and tissues is one of the most frequent, devastating, and costly problems in human health care. Tissue engineering is an multidisciplinary field that applies the

principles of engineering and life sciences toward the development of biological substitutes to restore, maintain, or improve tissue function [76]. In the tissue engineering paradigm, engineering and life sciences tools are combined to develop bioartificial substitutes for organs and tissues, which can in turn be applied in regenerative medicine, pharmaceutical, diagnostic, and basic research to elucidate fundamental aspects of cell functions in vivo or to identify mechanisms involved in aging processes and disease onset and progression (Fig. 1.3). The complex three-dimensional (3D) architecture and microenvironment in which cells are organized in vivo allows the crosstalk between different cell types and between cells and the ECM, the composition of which varies as a function of the tissue, the degree of maturation, and health conditions. In this context, 3D in vitro models can more realistically reproduce a tissue or organ than two-dimensional (2D) models, providing stimuli (e.g., soluble factors and physical strain) that strongly influence cell functions and gene expression profile. In the 2D setting essential environmental cues are not considered and the standardized culture conditions lead to accumulation of waste products in the culture medium, limited nutrient supply, and the lack of cell-specific mechano-stimulation that mimic the native environment. The lack of specific and unique culture conditions leads in loss of many of the requisite cell's phenotypic characteristic often necessary for their utility in predictive drug assays, and as a consequence of these non-physiological cell culture conditions, drug and therapy screening using the 2D setting in vitro mostly fail when tested in vivo (only 11.8% of drugs entering clinical trials become approved resulting in the average cost of ~$2.5 billion for each patented drug). This low efficacy in clinical translation is due in part also to animal disease models not truly replicating human diseases and to the differential drug response and toxicity between animals and humans. To this intent, essential premise is the availability of suitable in vitro and in vivo models, faithfully mirroring the disease phenotype.

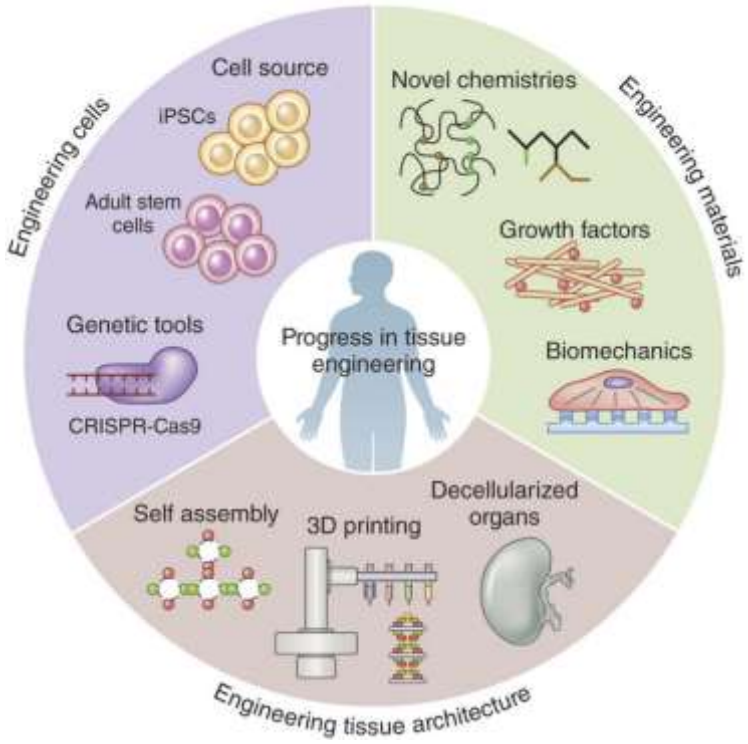

Fig. 1.3 Tissue Engineering approaches

(Source: Nat Protoc. 2016 Oct;11(10):1775-81. Doi: 10.1038/nprot.2016.123)

In the recent years, great attention was attributed to the use of primary myogenic cells obtained from patients' biopsy as cells source for cells therapy and regenerative medicine approaches, because they exactly display the pathological condition, permitting also to directly verify the outcome of any possible therapeutic approach. In vitro myogenic cells normally grown as a monolayer on flat stiff substrates, cells first need to proliferate and then differentiate forming multinucleated myotubes that in order to be functional and useful to drug screening, should be well organized and oriented to form a functional bundle and not randomly distributed in the plate. If heterologous cells expressing the protein of interest or that recapitulate phenotypically the disease may be useful and easy models to carry out high throughput screening processes in vitro, animal models are needed to evaluate primarily the functional outcome of any treatment. However, not always animal models display all the pathological features present in the human condition, , or they can develop a more severe phenotype so that they are difficult to generate and care for, and often die prematurely [77]. Sometimes animal models may fail in developing the disease despite carrying the amino acid substitutions responsible for the most frequently reported defects in humans, like in the case of SG-KO mouse lines [78, 79]. Furthermore, several animal models may be useful to understand some aspects of the pathogenic mechanism of the

disease or to test some therapeutic approaches but are insufficient to unveil the entire complexity of the disease pathogenesis. 3D in vitro models can overcome the limitations of animal models and reduce the need for in vivo tests, according to the "3Rs" guiding principles for a more ethical research ("3Rs" stand for Replacement, Reduction and Refinement. Replacement alternatives refer to methods which avoid or replace the use of animals). Soon, 3D in vitro tissue-engineered models are expected to become useful tools in the preliminary testing and screening of drugs and therapies and in the investigation of the molecular mechanisms underpinning disease onset and progression filling the gap between in vitro drug screening and clinical translation [80].

Over the last 30 years, in vitro tissue-engineered skeletal muscle models have progressed significantly to replicate key aspects of skeletal muscle function including generation of contractile force, regeneration from toxin injury, and physiological pharmacological responses.

To date, scaffold-based and scaffold-free approaches have been the two major strategies for engineering 3D skeletal muscle tissues. Scaffold-based approaches consist in the generation of biologic constructs embedding and culturing cells within a 3D matrix that serves to replicate the native mechanical environment. Scaffold-free approaches involve seeding myogenic cells and fibroblasts in 2D monolayers under conditions that promote the synthesis of sufficient ECM followed by cell self-assembly into a 3D construct. While synthetic polymers such as polyurethane, poly-L-lactic acid, and poly (lactic-co-glycolic) acid can be used to generate 3D muscle tissues [81], the most common biomaterials used in scaffold-based approaches are collagen, fibrin and ECM derivates. Two fundamental goals in skeletal muscle tissue engineering are the parallel alignment of myotubes and a high degree of muscle maturity, since without these conditions, the 3D construct results non-functional. Mechanotransduction plays a central role in myogenic differentiation, and mechanical stimulation has been demonstrated to induce cellular alignment along the axis of strain and to stimulate muscle growth in vitro [40, 41].

Recent advances in the optimization of 3D culture conditions and human pluripotent stem cells (hPSCs) technology have permitted the generation of the first functional tissue-engineered human muscle constructs made of primary myoblasts or fusion-competent hPSC-derived muscle progenitors. Maffioletti et al. showed the generation of 3D engineered skeletal muscle from human hPSCs derived from DMD, limb-girdle and muscular dystrophies patients. They induced 3D skeletal myogenic differentiation of iPSCs using hydrogels under tension to provide myofibers alignment [82]. Additionally, smaller scale muscle on-a-chip platforms offer the capability to study muscle biology and drug screening in a high-throughput fashion manner.

1.3.2 Cell sources for human skeletal muscle engineering

The ability to generate engineered muscle tissues from human primary and pluripotent stem cells can enable personalized tests of human muscle function and metabolism in response to various drugs in vitro. In preclinical pharmacological tests, these tissues must respond to drugs in a reproducible manner comparable to the native muscle.

Primary human muscle stem cells

Since multinucleated and differentiated cells within mature myofibers are post-mitotic, SCs represent the only source of expandable primary myogenic cells in skeletal muscle. Once isolated, primary human myoblasts rapidly proliferate in high serum media, and readily fuse to form multinucleated myotubes when switched to low serum media and contact inhibition. This cell source can be isolated easily from patient biopsy and represents the most faithful mixture of cells that recapitulate the heterogenicity of subtypes present in the muscle tissue [83]. However, with serial passaging these cells become senescent: proliferation rate decreases, DNA damage accumulates, ability to terminally differentiate decrease, and potential to engraft into the SC niches in vivo is lost [84, 85].

Human pluripotent stem cells (hPSCs)-derived myogenic cells

To overcome the passaging limitations and ethical considerations of utilizing primary cells from healthy donors and patients, methods have been developed to generate MPCs from human pluripotent hPSCs. The hPSCs, including human embryonic stem cells (hESCs) and induced pluripotent stem cells (hiPSCs), can serve as near-unlimited cell sources capable of differentiation into all three germ layers of the early embryo. In the past 10 years, significant progress has been made in the derivation of hPSC-MPCs for use in cell-based therapies and to study muscle development and disease. Nowadays, despite the big efforts to achieve an optimized and clinical accepted protocol to obtain myogenic committed cells from hPSCs, there are still important improvement to be made. The ideal cell population, either for cell therapy and tissue engineering approaches, should be easily accessible, obtainable in high amount and not dangerous for human health (non-teratogenic, possibly autologous rather than allogenic), able to proliferate and differentiate (under controlled stimuli) and to retain this ability during time.

Initially regenerative medicine focused its effort especially on cell therapy, finding solutions to deliver cells either systemically or locally to mediate injury repair [86].

The delivery of cells, concerning the skeletal muscle compartment, in the proper anatomical location face therapeutic limitation. Several obstacles related to cell therapy approach have been observed, such as the poor migration abilities of injected cells, low cells engraftment and retention into the host tissue and also the undesired off target engraftment when the systemic delivery is used [87].

2. Aim

The principal aim of my project is to generate *in vitro* a 3D model of diaphragm-like muscle tissue starting from decellularized extracellular matrix (dECM) and human skeletal muscle cells, as new approach for modelling advanced personalized therapy models, and the production and characterization of a clinically relevant dECM patch as new biocompatible solution for CDH (Fig. 2 AIM). Diaphragm is one of the most affected muscles in muscular dystrophies; among all the subtypes, we specifically investigated the limb-girdle muscular dystrophy, in which the different isoforms of sarcoglycans is missing. In the sarcoglycanopathies, the mutated proteins responsible for the development of the diseases are key elements of the DAPC complex.
In this project we are aiming at:

- Characterize and compare decellularized ECM from healthy and αSG KO mice;

- Set-up of bioreactor culture, specifically designed for diaphragm-like muscle tissue constructs, using different pattern of mechanical strain protocols, in order to physiologically stimulate human cells (myogenic progenitors and fibroblast) to recellularize the dECM in the proper manner, boosting cells engraftment, disposition and orientation, and finally differentiation and maturation of the engineered diaphragm-like muscle;

- Analyze the crosstalk between human cells and healthy and pathological derived diaphragmatic dECM;

- Set-up and optimization strategy to produce a clinically relevant dECM patch derived from porcine native diaphragm, to propose a new biocompatible solution for the treatment of large CDH defect.

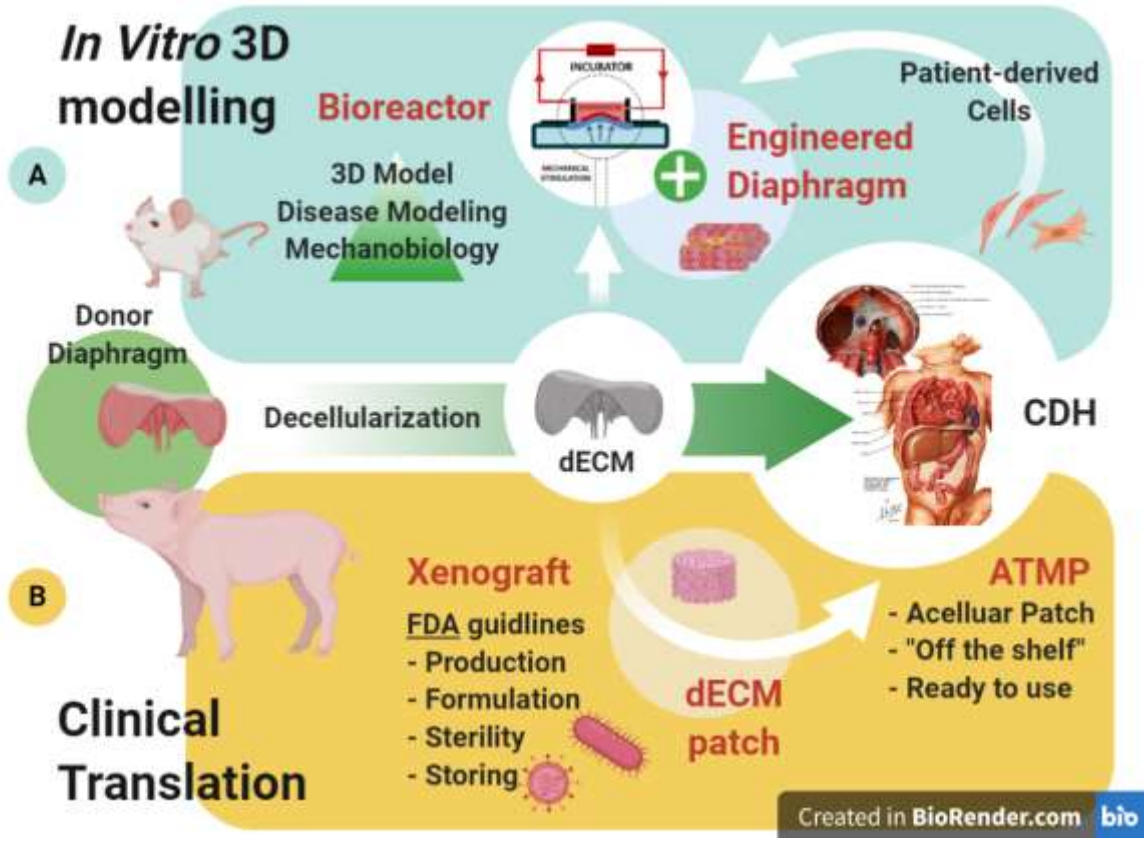

Fig. 2 Tissue engineered strategy for CDH.

(A) Starting from decellularized extracellular matrix (dECM) obtained from mouse donor, we developed an in vitro 3D model combining dECM with human skeletal muscle cells and bioreactor platform, as new approach for modelling advanced personalized therapy models.

(B) We characterized, following FDA guidelines, the dECM obtained from piglet donor as a new clinically relevant and biocompatible solution for CDH.

3. Material and Methods

3.1 Mouse diaphragm tissue collection

Animal husbandries were carried out in accordance with University of Padua's Animal care and Use Committee (CEASA, 1103/2016-PR approved on 15th November 2016) and were communicated to the Ministry of Health and local authorities in accordance with the Italian Law on the use of experimental animals (DL n. 16/92 art. 5). The animals used as healthy diaphragm donors were 12 weeks-old wild type (wt) C57BL/6j male and female; animals used as pathological diaphragm donors were 12 weeks-old αSG KO male and female, thanks to the collaboration with Professor Doriana Sandonà of Biomedical Sciences Department, University of Padua. Once sacrificed the mouse, the diaphragm was harvested carefully to preserve the rib cage, then washed and preserved in sterile and deionized water at 4°C, for 24-48 hours previous to decellularization process.

3.2 Mouse diaphragm decellularization by diffusion

Decellularization was performed using a detergent-enzymatic treatment (DET) in immersion and agitation. Specifically, 4% sodium deoxycholate (SDC; Sigma-Aldrich) was used as detergent and deoxyribonuclease I (DNase I; Sigma-Aldrich) as nuclease. Diaphragm muscles obtained from healthy or pathological mice were washed in sterile 1X phosphate buffered saline (PBS; Sigma-Aldrich) when collected. A DET cycle consisted of 3 steps:

- 40 ml of sterile and deionized water at 4°C, for 24 hours;
- 30 ml of 4% SDC for 4 hours at room temperature (RT) and in gentle agitation; 3 washing steps with sterile and deionized water;
- 40 ml of 2000 kU DNase I in 1 M NaCl (Sigma-Aldrich) for 3 hours at RT and in gentle agitation.

We performed 3 DET cycles to reach complete decellularization for mouse diaphragm. Then, matrices were washed for at least 3 days in 1X PBS and 3% penicillin/streptomycin (P/S; Gibco-Life Technologies).

3.3 Piglet and porcine diaphragm tissue collection

Piglet (*Sus scrofa domesticus*) from the 'Pietrain' breed were used as healthy diaphragm donors. Piglets up to 3 kg in weight were euthanized via blunt trauma once the criteria outlined by the JSR veterinary advisors had been met (following the UCL guidelines). Once sacrificed, the animals were transported to the lab via courier and the diaphragm was harvested immediately on arrival (within 6 h of euthanasia) then it was immediately decellularized or stored at – 80° C.

Porcine farm animals (25 kg) sacrificed for the food market were used as diaphragm donors that undergo decellularization by diffusion. Once harvested in the lab, the diaphragm was disinfected (10% Betadine), cleaned and stored at – 80° C.

3.4 Piglet diaphragm decellularization by perfusion

The whole diaphragm was harvested and excise from the rib cage. Cannulation of inferior vena cava (IVC) was performed using fitting tube adaptor and surgical stiches to ensure no leak in both diaphragm side. Perfusion was performed at 2ml/min, inside sterilize bottle in an interconnected system of perfusion run by peristatic pump. To achieve decellularization we perform 3 DET cycle consisted of:

- sterile and deionized water at 4°C, for 24 hours;
- 4% SDC for 4 hours;
- Washing steps with sterile and deionized water for 2 hours;
- DNase I in 1 M NaCl (Sigma-Aldrich) for 3 hours;

3.5 Porcine diaphragm decellularization by diffusion

Porcine native diaphragm was thaw at + 4°C, at least 6 hours before starting decellularization. After defrost process and before decellularization, the native diaphragm was dissected in patches of defined size: 3 x 4 cm, with a mean thickness of 0.5 cm (Fig. 4.12 A). The epimysium was dissected from diaphragmatic muscle, only a portion of the central tendon was maintained as useful surgical stitch area. Native ECM patches were decellularized with 4 DET cycles by

agitation/diffusion as reported in 3.2 section, changing only the solution volume (about 100 ml). The average weight of each single dECM was around 6 gr.

3.6 dECM storage for subsequent recellularization

dECM after decellularization were kept at + 4°C, ready to be used for recellularization within 2 weeks; 1X PBS supplemented with 3% of P/S was changed every 3 days in order to maintain antibiotic coverage. Otherwise, dECM have been store in liquid nitrogen with freezing medium. Specifically, dECM were immersed in 1 ml of freezing medium (10% DMEM high glucose (4.5 g/l D-glucose, Gibco-Life Technologies), 20% dimethyl sulfoxide (DMSO; Sigma Aldrich) and 70% fetal bovine serum (FBS; Gibco-Life Technologies), slowly cooled in cryoboxes overnight, and then transferred to liquid nitrogen. Stored dECM were defrosted the day before performing experiment, washed in 1X PBS supplemented with 3% P/S and preserved at 4° C.

3.7 ECM components quantification

Wet samples for quantification were snap frozen before use. Collagen, sulphated glycosaminoglycan (sGAG) and elastin content on decellularized diaphragms were quantified using respectively the SIRCOL collagen assay, Blyscan GAG Assay Kit and Fastin Elastin Assay Kit (all from Biocolor, UK) under manufacturer's instruction.

3.8 Gamma irradiation

Piglet diaphragm dECM derived from perfusion decellularization were packed in sterilization pouches and irradiated with a dose of 15 kGy at room temperature, using a 60Co gamma-ray source (Isotron, Berkshire, UK). Samples were exposed to the source on a continuous path for a period of 10 hours.

3.9 Peracetic Acid (PAA) treatment

Porcine diaphragm dECM derived from diffusion decellularization, following incubation with 3% antibiotic/antimycotic solution, were treated with 1% peracetic acid (PAA) solution for 1h or 3h and then washed with several cycles of sterile PBS until lyophilization.

3.10 Lyophilization

Porcine dECM were cut to the dimension of a clinical relevant patch (3x4x0.5 cm) and then lyophilized by a -50°C vacuum freeze-drying instrument (FD-1 A-50, Beijing Boyikang Instrument Co., LTD, China) for 72h, then stored at room temperature or -20°C.

3.11 Bacterial contamination and titer measurement

Flasks containing dECM and bacteria were incubated for 21 hours. After incubation, surnatant was remove and replaced with fresh medium for other 24 hours. After incubation, surnatant was collect and diluted to quantify bacterial titer and dECM treated with terminal sterilization protocols.

3.12 Human skeletal myoblasts culture

Human skeletal myoblasts (HSkM) were purchased from Gibco-Thermo Fisher Scientific. Immortalized healthy human myoblast (AB678) were obtain thanks to the collaboration with Professor Doriana Sandonà of Biomedical Sciences Department, University of Padua**.** The seeding density adopted for 2D cultures was 5 x 10^5 cells in a 150 mm x 15 mm NTC Petri dish; cells were seeded and cultured in Proliferating Medium (PM; DMEM low glucose, 20% FBS (Fetal bovine serum), 10^{-6} M dexamethasone (Sigma-Aldrich), 10 mg/mL basic fibroblast growth factor (bFGF) (R&D System), 10 mg/mL insulin (Humulin-Eli Lilly), 1 % P/S) , at 37°C, 5 % CO_2, with an oxygen tension of 9% in hypoxia incubator chamber (Don Whitney Scientific). In order to detect the presence of proliferation markers and determine growth characteristics, respectively 5 x 10^3 and 3 x 10^3 cells were seeded in a 96-well NTC plate in PM and cultured for 24 hours and 5 days. For myogenic differentiation, hSkMC at confluence were cultured for 96

hours in fusion medium (FM) composed of AlphaMEM (Gibco-Life Technologies) supplemented with 2% HS, 10 μg/ml insulin, 1% P/S.

3.13 Human fibroblasts culture and expansion

The human fibroblasts (hFb) culture was employed to obtain a mixed cell population combined with HSkM. Human fibroblasts were purchased from Sigma Aldrich, and cultured in fibroblast medium (DMEM high glucose (4.5 g/L D-Glucose), 20% FBS, 1% P/S and 1% Glutamine), with an initial seeding density of 1 x 10^6 cells in a T75 flask or 3 x 10^5 in a T25 flask.

3.14 Flow cytometry analyses

Cell surface antigen expression was analyzed by flow cytometry using cultivated cells after detachment by trypsin-EDTA treatment (passages 3 to 5). Briefly, cell suspensions were incubated with 5 μL of antibody for 20 min at 4 °C in the dark. After a wash step, the cells were resuspended in 1X PBS; acquisition and analyses were performed using Accuri C6 flow cytometer (Becton Dickinson). The antibodies used were: CD34 FITC, CD56 PE (both from BD Bioscience). 7-aminoactinomycinD (7AAD) was used as viability marker.

3.15 Bioreactor design, modeling and manufacturing

The bioreactor design methodology used is a numerical modelling based on the finite element method (FEM) approach to estimate the correct structural behaviour of the system and to size each single component. The main concept of the bioreactor system is explained in Fig. 3.1 and is composed of two principal components: an incubator bench unit and a motor bench unit.
In the incubator bench unit, the diaphragm is firmly placed upon the upper surface of an elastomeric membrane of polymethylsiloxane (PDMS) that is deformed under application of a hydrostatic pressure acting on its lower side. The deformation of the elastomeric membrane induces a deformation of the diaphragm that follows the membrane in its deformation, being largely softer. The hydrostatic pressure in the lower surface of the elastomeric membrane is induced through a hydraulic circuit connected to the motor bench unit. The motor bench unit consists in a double crankshaft system, moving two indenters and deforming two hydraulic

cameras, therefore generating the hydrostatic pressure into two distinct incubator bench units. Each pair of crankshafts is moved by a servomotor that, in turn, is controlled with a Genuino board. Finally, the Genuino board is interfaced with a Personal Computer. A software specifically developed controls the mechanical cycles in terms of strain magnitude induced to the diaphragm tissue, frequency and overall time of application of the mechanical stimulus. The incubator bench units are placed in a light hypoxia sterile incubator, under controlled conditions of oxygen, temperature and relative humidity.

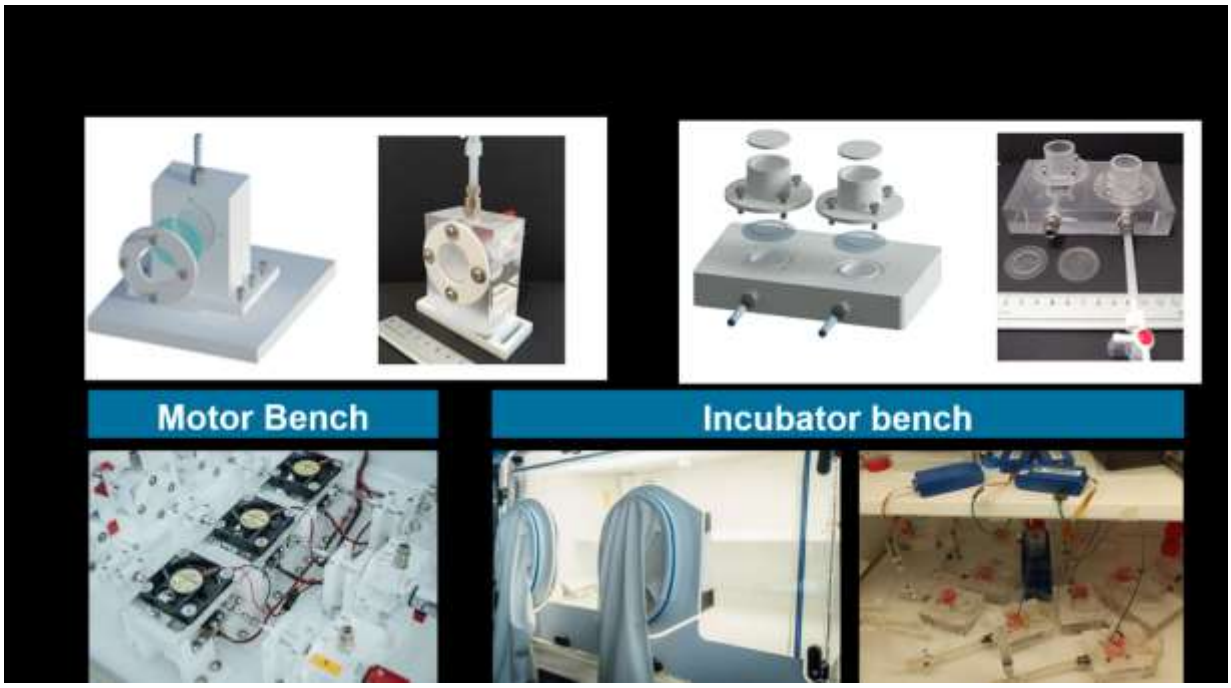

Fig. 3.1 Bioreactor components. *(A) CAD 3D modelling and manufactured units;*
(B) representative pictures of motor bench, light hypoxia incubator and bioreactors experiments.

We designed the whole system to have at disposal three servomotors. Each servomotor moves two crankshafts and can induce a cyclic pressure on two distinct incubator bench units, at the same time. Therefore, the motor system moves six incubator bench units. This makes it possible to test six sample in the same environment conditions (temperature and relative humidity) and changing the type of mechanical stimulus. This solution has two advantages: i) to reduce the variability of the environmental conditions; ii) to reduce the global time of experimental testing, making it possible to test multiple samples at the same time. The software developed to control the system has an intuitive graphic interface to easily set overall time of stimulation, magnitude of strain induced on the diaphragm and frequency of cycles. The main data of each experiment

(e.g. total cycles, total time, etc.) and possible anomalies occurred during a test are recorded in a file. To exert slow stress ramp, we used a programmable syringe pump that can be swap with the hydraulic motor bench unit input in the interconnection with the hydraulic circuit. We developed different tests, applying high frequency mechanical (up to 60 cycles/minute) for an overall time of five days, verifying the good reliability of the system. We developed also static tests to verify the correct deformation of the elastomeric membrane of the incubator bench units, by measuring the amount of liquid volume moved by the membrane and comparing it with the expected liquid volume movement as a function of the indenter displacement.

3.16 Recellularization procedures

Bioreactor

Prior to recellularization, mouse dECM diaphragms were rinsed with 0.1% PAA for 30 minutes in gentle agitation for disinfection. Thereafter, the vertebral column and crural muscle were cut off from each dECM and the ribcage trimmed to a thin layer and sewed, in order to fix the diaphragms on the PDMS membranes through stiches. Once the diaphragms were ready for recellularization, hSkMC and hFb (separately expanded for 3 to 10 passages) were mixed in a ratio of 85%-15% and resuspended in 40 µL of 13% Collagen I (Sigma-Aldrich), 10% Fibronectin (Sigma-Aldrich), 20ng/mL IGF-1 (ImmunoTools) in PM. The mix was injected at a density of 3 x 10^6 total cell per scaffold, performing 4/5 injections all around dECM scaffold. After 2 hours from the injection, the constructs were transferred in the bioreactor support and 2 mL of PM were added, the rest 3 mL were added after other 1.5 hours. The PM was maintained for 4 days, and then changed according to the glucose consumption every other day before being replaced by FM for 3 days. PM was used for the rest of the culture period. The diaphragm-like constructs were analyzed after 3, 7, 11 or 14 days of culture.

Porcine dECM

Porcine-derived dECM patches were cut in define sized (1x0.5x0.5 cm), then lyophilized and store at – 20° C prior to recellularization. Then a mixed population (cell density: 4 x 10^6) of hSkMC (85%) and hFb (15%) were mixed in a ratio of 85%-15% and resuspended in 150 µL of 13% Collagen I, 10% Fibronectin 10% IGF-1 in PM, and injected directly within the scaffold with an insulin syringe (30G). We used 150 µL of the same combination of factor to resuspend

and vehicle the cells within the lyophilized dECM in order to re-hydrated completely the scaffold area. The constructs were cultivated in 24 well culture dish with 2 ml of proliferating medium until day 4 to switch then to the differentiation medium until day 7.

3.17 Freezing process of fixed samples

All the tissue samples were fixed with 4% paraformaldehyde (PFA) (Sigma-Aldrich) for 1 hour at 4°C. The samples dehydrated with a sucrose gradient (10%, 15% and 30%; Fluka) were then included in cryostat embedding medium O.C.T. (Kaltek) and frozen in liquid nitrogen using isopentane (Sigma-Aldrich). The frozen tissues were sectioned with cryostat (Leica CM1520) in sheets of 6-10 µm.

3.18 Histology

Frozen tissue sections were stained with H&E kit for rapid frozen section and with Masson's trichrome (MT) with aniline blue kit (all from Bio-Optica, UK) under manufacturer's instruction.

3.19 Immunofluorescence analysis

For immunofluorescence analyses, tissue slides were permeabilized with 0.5% Triton X-100 (Fluxa) in 1X PBS for 10 min at RT. After, the samples were rinsed in 1X PBS for 5 min and then saturated with 10% horse serum (HS), goat serum (GS) or mouse serum (MOM) (Gibco-Life Technologies) in 1X PBS for 10 to 30 min, the different blocking condition was specifically optimized for specific antibodies, following manufacturers' guidelines. Another washing step in 1X PBS for 5 min was done. The samples were then incubated with primary antibody for 1 hour at 37°C or overnight at 4°C. After a washing step with 1X PBS, they were incubated with labelled secondary antibody for 1 hour at 37 °C. After the last washing step with 1X PBS, nuclei were counterstained with fluorescent mounting medium plus 100 ng/ml 4',6-diamidino-2-phenylindole (DAPI: Sigma-Aldrich).

For immunofluorescence analyses of cell cultures, after 72 hours in 96-wells nonTC plates proliferating cells were fixed in 4% PFA for 10 min at 4 °C, then rinsed in 1X PBS and

permeabilized with 0.5% Triton X-100 in 1X PBS for 10 min at RT. Non-specific interactions were blocked with 10% HS for 30 min at RT. After washing cells in 1X PBS, they were incubated with primary antibodies for 1 hour at 37 °C or following manufactory guidelines. Cells were then washed twice with 1X PBS and incubated with labelled secondary antibodies for 1 hour at 37°C. After double washing with 1X PBS, nuclei were counterstained with HOECHST (Life Technologies, dilution 1:10.000) for 15 min at RT. For differentiation analyses, human MPCs were seeded in 24-wells TC plates (15.000 cells/well), expanded in PM for 72 hours, and differentiated with FM for 96 hours. The fixation and staining procedures were the same described for proliferating cells. To quantify myoblast fusion, the myogenic index (MI), defined as the number of nuclei residing in $MYHC^{+}$ cells containing three or more nuclei divided by the total number of nuclei, was calculated from 5 random fields of each sample.

3.20 Whole mounting immunofluorescence

For whole mounting immunofluorescence staining, native or dECM mouse diaphragm were stretched in sylgard-coated dish and fix in 4% PFA at 4°C for 1 hour. After rising in 1X PBS, the tissue was permeabilized and block for 1 hour in triton 0.5% X-100, containing 2% BSA, 4% GS). Then after 2 washing in 1X PBS the sample was incubate overnight at 4°C with primary antibodies diluted in 2% BSA. It essential to force by pipetting the antibody solution into the muscle to provide good access into the tissue. After primary incubation, the sample was rinsed in 1X PBS and incubate for 1 hour at room temperature with secondary antibodies. Tissue samples was put on tissue slide, counterstained with DAPI and securely close with coverslip.

3.21 Western Blot

Total proteins were extracted with RIPA lysis buffer (89900, Thermo Scientific) supplemented with 1X Protease InhibitorÐComplete ULTRA tablets mini (5892791001, Roche) and 1X Benzonase nuclease HC (712063, Millipore) for 1 hour at 4°C. Equal amounts of total cellular proteins were resolved on NuPAGE1Novex14±12% Bis-Tris Protein Gels (NP0336BOX, Thermo Fisher Scientific) and transferred to nitrocellulose membranes (iBlot, Thermo Fisher Scientific) following the manufacturer's instructions. Membranes were then blocked in Odyssey Blocking Buffer (927-4-0000, Li-Cor) for 1 hour at room temperature. Incubation with primary

antibodies were carried out at 4°C overnight in Odyssey Blocking Buffer. The following antibodies were used: rabbit anti-βSG (dilution 1/100, Sigma) rabbit αSG (dilution 1/1000, Abcam) rabbit anti-laminin (dilution 1/100, Sigma), mouse anti-ACTA (dilution 1/100, Sigma) and mouse anti GAPDH (dilution 1/100, Sigma). After 1-hour incubation with donkey anti-rabbit 680 antibody (EuroBio) at room temperature, proteins were detected by fluorescence (Odyssey, Li-Cor) following the manufacturer's instructions.

Antibody	**Dilution**	**Manufacturer**
Laminin (Rabbit)	1:150	Sigma-Aldrich
Lamininα2 (Rat)	1:100	Sigma-Aldrich
Collagen 1 (Rabbit)	1:100	Abcam
Collagen 4 (Rabbit)	1:100	Abcam
αSG (Rabbit)	1:1000	Abcam
KI67 (Rabbit)	1:100	Abcam
MYF5 (Rabbit)	1:80	Santa Cruz
MYOD (Mouse)	1:50	Dako
MYF5 (Rabbit)	1:80	Santa Cruz
Myogenin AF488	1:80	Invitrogen
MYHC (Mouse)	1:100	R&D Systems
ACTA (Mouse)	1:100	Sigma-Aldrich
Muscle Actin AF488	1:100	Invitrogen
Phalloidin AF488	1:1000	Abcam
αSMA (Mouse)	1:100	Abcam
TE7 (Mouse)	1:100	Millipore
Anti-Rabbit 488	1:200	Life Technologies
Anti-Rat 488	1:200	Life Technologies
Anti-Rabbit 594	1:200	Life Technologies
Anti-Mouse 594	1:200	Life Technologies
Anti-Rat 568	1:200	Life Technologies

Table 1. Antibodies used for immunofluorescence and western blot analysis

3.22 Microscopes and imaging system

Phase-contrast images were collected using an inverted microscope (Olympus IX71). Immunofluorescence analyses were performed using a fluorescence inverted microscope (Leica B5000) or Zeiss Axio Observer (LMS 800).

3.23 Transmission electron microscopy (TEM)

dECM for TEM were fixed in 4% PFA for 1 hour and then with 0.25% glutaraldehyde in 0.1 M sodium cacodylate buffer overnight. After wash, small portions were post-fixed in osmium tetroxide 1% for 1 hour at 4°C and then embedded in Epon 812 resin. Ultrathin sections, obtained with a Reichert-Jung Ultracut ultramicrotome, were recovered on slot grids and counterstained with uranyl acetate and lead citrate. The samples were examined with a FEI Tecnai G2 transmission electron microscope operating at 100 kV. Images were captured with a Veleta (Olympus Soft Imaging System, Münster, Germany) digital camera.

3.24 Scanning electron microscopy (SEM)

dECM for SEM were fixed with 2% glutaraldehyde in 0.1M phosphate; after was, small segments of approximately 1 cm length were cryoprotected in 25% sucrose, 10% glycerol in 0.05 MPBS (pH 7.4) for 2 hour, then fast frozen. Images were recorded with a Jeol 7401 FEG scanning electron microscope.

3.25 Statistical analyses

Statistical analyses were performed with GraphPad software 6.2. The data are presented as mean ± SEM. Differences between data groups were evaluated for significance using the unpaired Student's t-test. P-values indicated on figures are * = $p < 0.05$; ** = $p < 0.01$; *** = $p < 0.001$.

4. Results

4.1 Healthy and pathological dECM characterization

Recently we characterized the diaphragm dECM obtained from healthy mouse. dECM possesses morphological, biochemical and biomechanical characteristics similar to those of the fresh native tissue [88]. After decellularization process, the main ECM proteins are well preserved, and in the proper anatomical disposition, with the overall 3D architecture well maintained, as shown by whole mounting IF analysis (Fig. 4.1 A) of native and decellularized ECM, where DAPI staining demonstrated nuclei removal after decellularization but preservation within the dECM of structural and tissue specific proteins such as muscle Actin, Laminin and MYHC (Fig. 4.1 B).

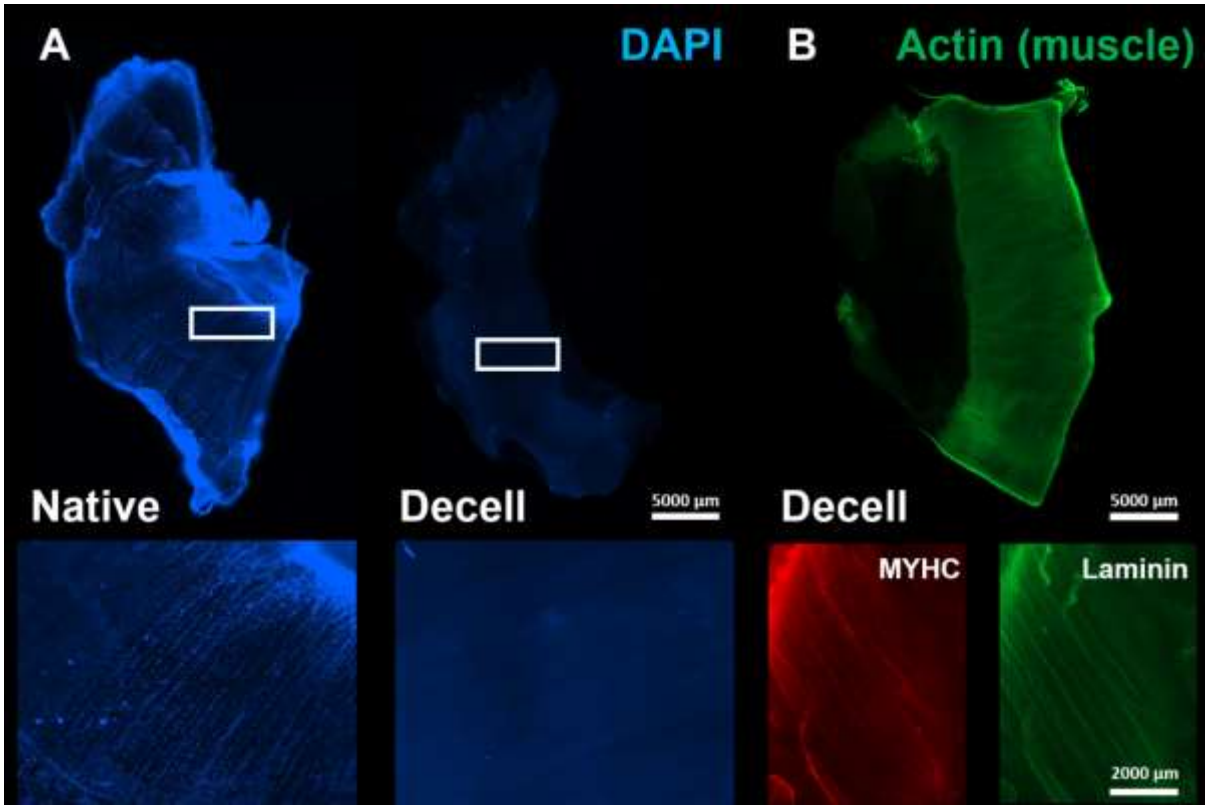

Fig. 4.1 Decellularization efficiency and ECM preservation of healthy dECM

(A) Evaluation of decellularization efficiency by whole mounting immunofluorescence of nuclei, stained with DAPI (blue), between native and dECM emi-diaphragm. (B) Emi-diaphragm dECM whole mounting immunofluorescence of muscle actin, and representative images of MYHC and Laminin whole mounted sections.

In order to generate a pathological diaphragm-like tissue, we first characterized and compared the pathological dECM obtained from αSG KO mice with the healthy one. Both dECM after characterization will be used as scaffold for immortalized healthy myogenic cell seeding.
In Fig. 4. 2 it is reported the immunofluorescence analysis of healthy native ECM compared with healthy and αSG KO derived dECM.
It is possible to observe that specific ECM collagens and Laminins are preserved and located around each single muscle fiber. In healthy dECM the αSG protein is preserved; on the contrary, as expected, the αSG KO derived scaffold is positive for all the tested ECM proteins, but is missing the αSG. Moreover, inside muscle fibers some functional muscle proteins such as muscle Actin are maintained. This result confirmed the goodness of our decellularization protocol, able to preserve several ECM proteins (i.e. collagens, laminins) and consequently the biological features of the native tissue, giving us the chance to obtain dECM derived scaffold with unique and preserved ECM composition from healthy or pathological skeletal muscle tissue.

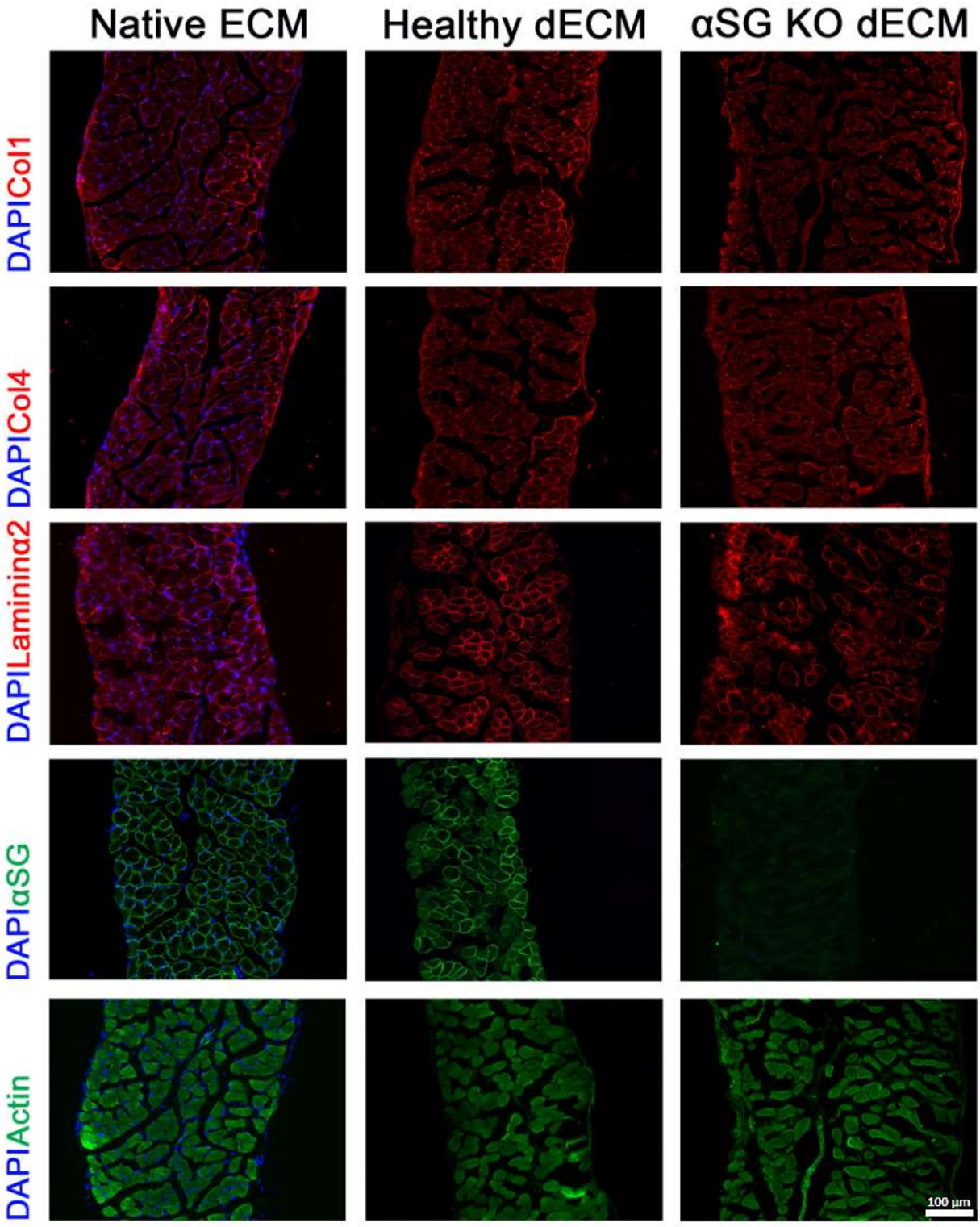

Fig. 4.2 Comparison of healthy and pathological dECM.

Comparison of healthy native diaphragm vs healthy dECM and αSG KO dECM derived matrix. Col1, Col4 and Laminin α2 are shown in red, αSG and muscle actin in green, nuclei counterstained with DAPI (blue) (scale bar = 100µm).

4.2 Engineered diaphragm-like tissue construction

4.2.1 Cell source for recellularization

As cell source to performed recellularization procedures, based on literature findings [57, 89] and on our previous results [90], we utilized a mixed population comprehensive of myogenic progenitors and fibroblasts. This mixed population, indeed, shapes up to be a good combination to favour myoblast migration and distribution, and reach a complete scaffold repopulation after cell injection. We used commercially available cell lines rather than primary human MPCs in order to investigate the proper dynamic protocol to mimic and recapitulate skeletal muscle development before using patient derived cells that are currently the best source. In this experimental setting, we used human skeletal muscle cells (hSkMC) expanded up to 10 passages and characterized by good proliferation rate (Ki67: 25.4±5.8%), expression of myogenic markers (MYOD: 16.4±7.7%; MYOG: 12.2±6.8%; CD56+: 97.5%) and differentiation capability (Myogenic index: 83.9±9.3%). Together with hSkMC, human fibroblasts (hFb), characterized by the expression of TE7 (93.7±8.4%) and alpha smooth muscle (αSMA, 61.5±29.2%) markers (Figure 4.3 A-C), were used. These two populations where co-seeded in a proportion of 85% of hSkMC and 15% of hFb, based on literature [57][89] and our previous experience [90]. These mix population shapes up to be a good combination to favour myoblast migration and distribution and reach a complete scaffold repopulation after cell injection. Co-culture experiments using standard 2D cultures demonstrated the ability to maintain unaltered this proportion during the culture period, suggesting a balanced proliferation between the two cell lines (Fig.4.3 D).

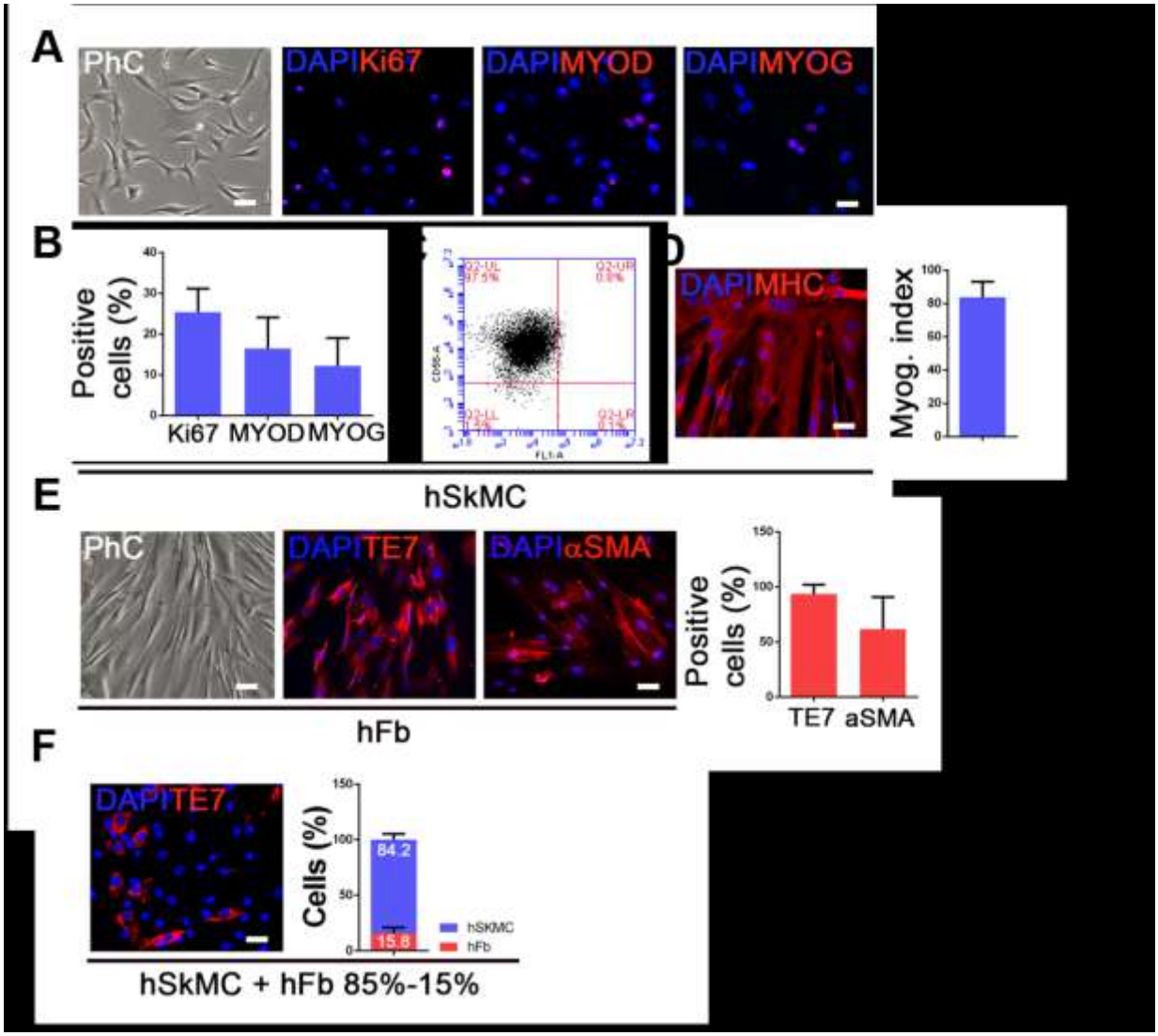

Fig. 4.3 Characterization of hSkMC and hFb used for subsequent recellularization experiments. *(A) phase contrast and immunofluorescence representative images of hSkMC labeled for Ki67, MYOD and MYOG marker (red) and (B) relative quantification. (C) Cytofluorimetry analysis of CD56 for cultured hSkMC. (D) Myogenic differentiation index quantification. (E) hFB phase contrast and immunofluorescence images for hFb markers Te7 and αSMA, shown in red and relative quantification. (F) Co-culture quantification (scale bar = 50μm).*

To perform recellularization, we scale up our previous published protocol [90]. dECM ribcages were trimmed to a thin layer and sewed, in order to fix the dECM scaffold on 22 mm circular PDMS membranes. Then hSkMC and hFb were mixed and resuspended in 40 µL of 13% Collagen I, 10% Fibronectin, 10% IGF-1 in PM. We choose this mix of specific ECM component and growth factors as cell vehicle to stimulate engraftment and proliferation inside the scaffold. The mix was injected with a 33G needle within dECM scaffold at a density of 3 x 10^6 total cell. After 2 hours from the injection, the construct was transferred and secured in the bioreactor support. The diaphragm-like constructs were analyzed after 3, 7, 11 or 14 days of culture, following the culture protocol described in 3.12 section.
Moreover, cell cultures and recellularization experiments were carried out in light hypoxia conditions (9.5% O_2), since recapitulating the physiological low oxygen tension of native skeletal muscle environment. In both conditions, culture media was changed each other day or added each time the glucose sensor displayed a consumption greater than 0.5 g/L.

4.2.2 Bioreactor culture of engineered-like diaphragm

Given the peculiar diaphragm myofibers disposition and the need of forcing cell alignment following radial orientation, we designed and fabricated a diaphragm-specific bioreactor to radially stimulate diaphragmatic constructs with programmable and individually tunable control of strain parameters (Fig. 4.4 A). The aim was to increase cell engraftment, distribution and alignment inside the dECM scaffold performing radial and continuous tensile strain for several days and ameliorate construct maturity and functionality through the application of cyclic mechanical strain as training period. We performed in parallel static and dynamic experiments and evaluated the differences in terms of cell distribution, differentiation and maturation. This bioreactor takes into account diaphragm construct anatomy, shape, dimension and physiological stretching based on FEM analysis of mouse diaphragm deformation [91]. In the dynamic samples, two different mechanical stimulation protocols were applied:

Slow stress ramp – 48h post injection, diaphragmatic constructs were stimulated with a slow ramp from 0% to 10% of mechanical strain for 7h, followed by a resting period of 17. This stimulation protocol was applied for 5 days (from day 3 to day 7 of culture).

Training protocol – from day 8, a cyclic mechanical stimulation was applied with a protocol of 3 cycles/day of 1 beat/min for 10 minutes and 5% of mechanical strain. This protocol was used for 7 days (from day 8 to day 14).

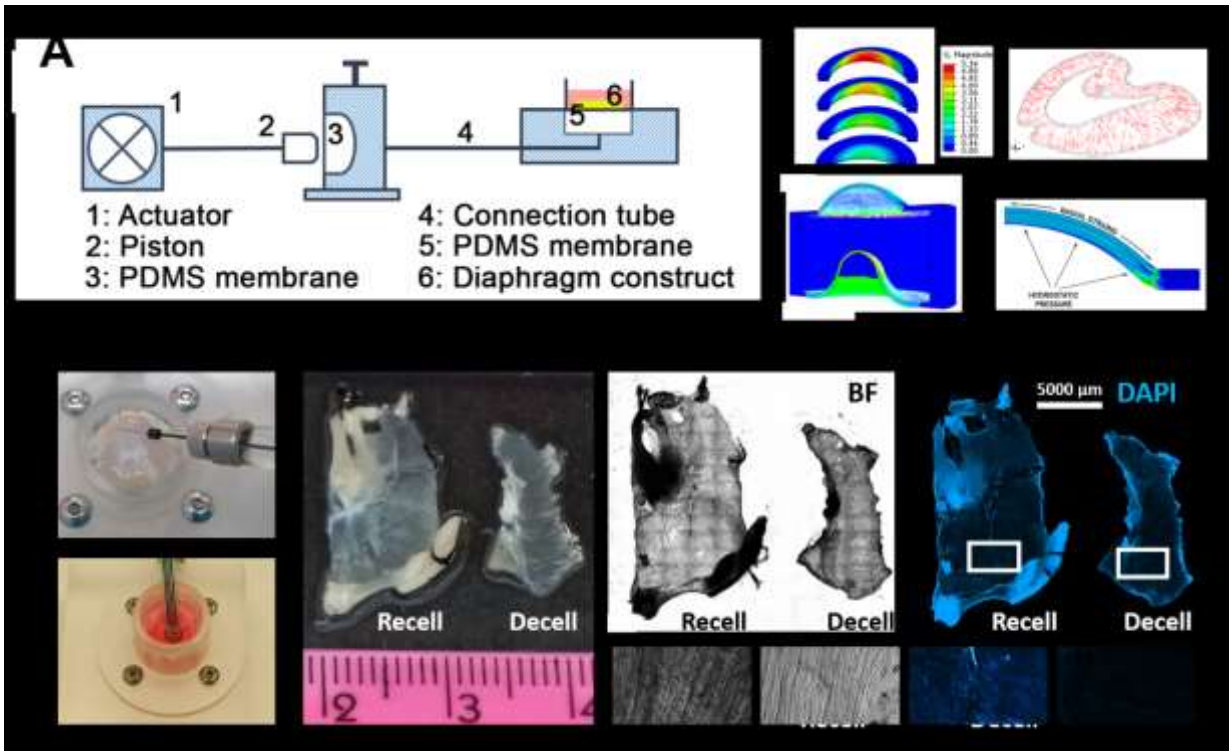

Fig. 4.4 Bioreactor design, validation and construction to recellularized diaphragm-like construct. *(A) Bioreactor scheme and Finite Element Modeling (FEM) of each single component. (B) Representatives pictures of cells injection and glucose biosensor inside the bioreactor chamber and comparison between recellularized samples at 7 days by bright field and whole mounting immunofluorescence.*

Recellularized samples from both macro- and microscopic point of view, appeared greatly different from decellularized scaffolds and more similar to fresh diaphragms (Fig. 4.4 B and 4.6 C). The effect of dynamic culture and application of mechanical stimulus was evident far from the beginning, influencing transversal cell distribution inside the construct despite an equal cell amount compared to static culture. Indeed, along the culture period, in the dynamic samples a statistically significant percentage of cells was found in the lower construct side (36.5±2.2%) in comparison with static culture (22.8±3.1%) (Fig. 4.5 A, B). Importantly, no difference in term

of total cell number was detected between the two culture conditions, indicating a general healthy and proliferating environment (Figure 4.5 C).

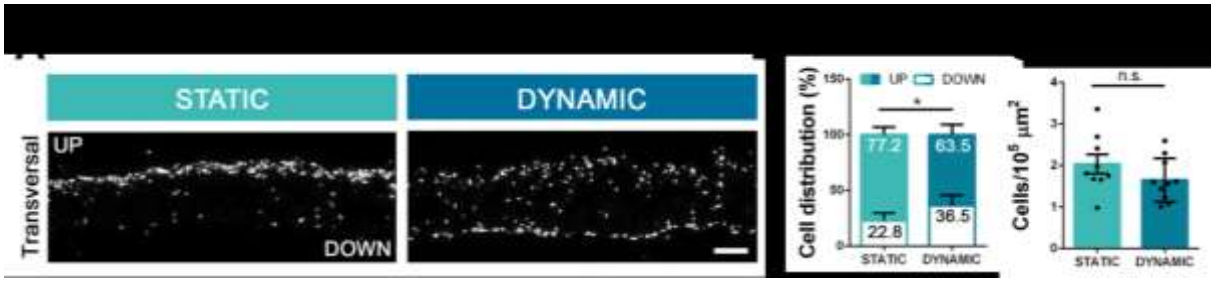

Fig. 4.5 Cells distribution within dECM in static and dynamic condition

Representative transversal images of static and dynamic construct at 7 days, cells are counterstained with DAPI (white), and relative (B) cells distribution in the upper (UP) or lower (DOWN) side of the dECM and (C) cells distribution among area in static vs dynamic culture (scale bar = 100µm).

4.2.3 Engineered diaphragm-like construct characterization.

Static and dynamic diaphragmatic constructs were maintained in culture for a maximum of 2 weeks, with analyses performed at different time points: 3, 7, 11 and 14 days. In the static samples, cell media were changed during the course of the experiment, as indicated in materials and methods section. For dynamic culture, instead, a sequence of two different mechanical stimulation protocols was also provided. Two days after cell seeding, we applied the first type of stimulation, using a slow stress ramp. This protocol was maintained for 5 days (until day 7 of culture). From day 8, we applied a training protocol, (Figure 4.6 A). Both static and dynamic constructs demonstrated a generally good appearance, with cells found on both scaffold sides, and a distribution that increased during the culture period, especially in the dynamic samples (Figure 4.5). Static and dynamic constructs were monitored for all the culture period through integrated glucose sensors [92], in order to follow glucose consumption and, indirectly, cell viability. Cell media were supplemented or changed every time the sensor indicated a consumption higher than 0.5 g/L (Figure 4.6 B). Proliferation rate was high in all the recellularized constructs (over 30%) until day 7, than decreased with a slightly different pattern: static samples reached a mean of 2.2±0.6% of Ki67+ cells after 14 days, whereas dynamic constructs showed a significant higher percentage of proliferating cell (6.4±0.8%) at the end of

the culture (Figure 4.5 E). Importantly, among all proliferating cells, at the beginning of the culture in both static and dynamic samples we observed a balanced proliferation rate between hSkMC and hFb; on the contrary, after 2 weeks of culture, in the dynamic samples a statistically significant higher number of hSkMC was detected compared to static constructs (53.3±14.0% Static; 71.9±7.1% Dynamic; Figure 4.6 F).

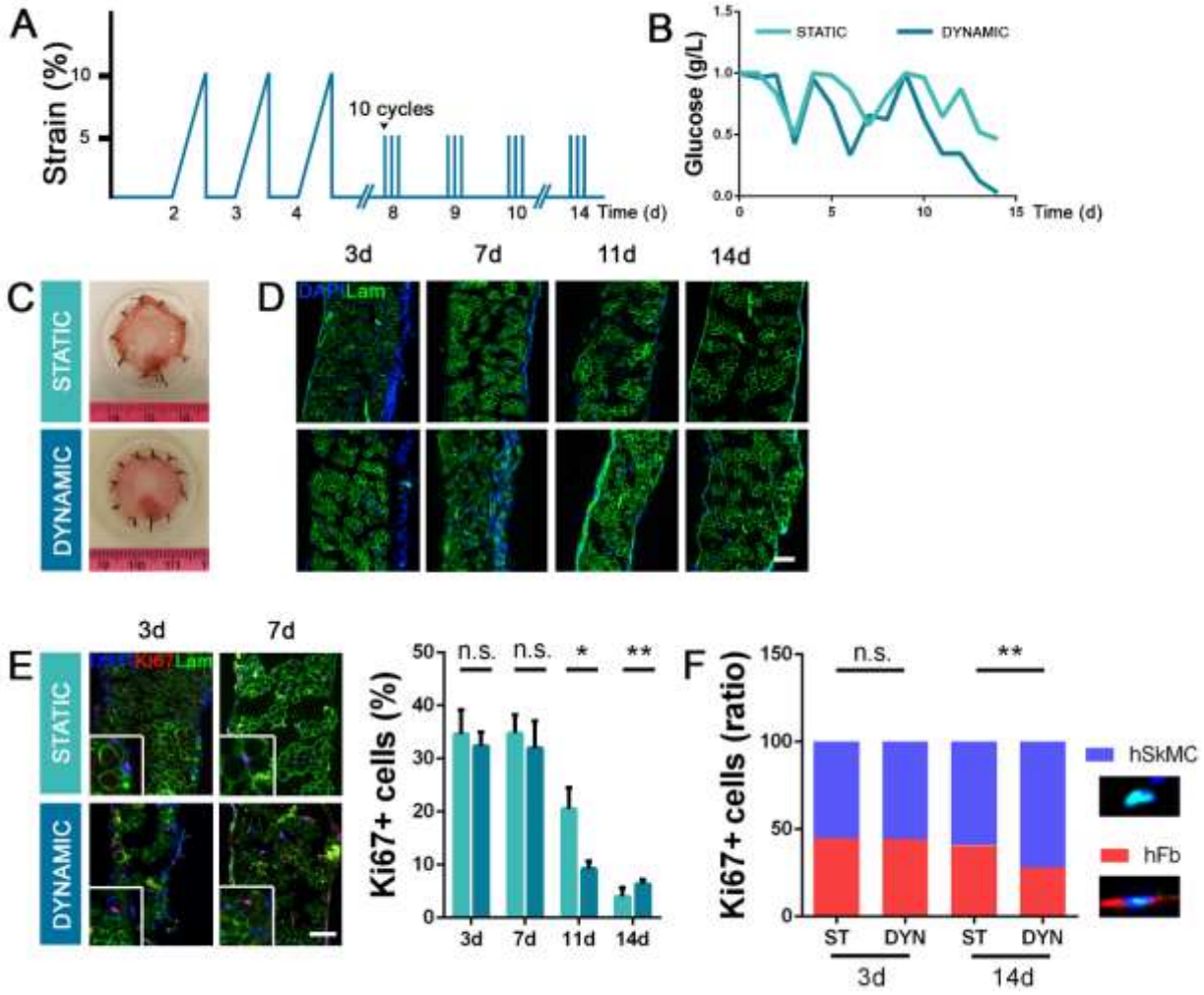

Fig. 4.6 Dynamic vs Static Bioreactor culture characterization

(A) Dynamic strain stimulation protocol applied to the dynamic culture and relative (B) glucose consumption monitored in real time during the culture, thanks to biosensor. (C) Macroscopic appearance of static and dynamic recellularized samples at 14 days. (D) Immunofluorescence of Laminin (green) and nuclei (DAPI) to evaluate cell distribution during time. (E) Immunofluorescence of proliferating cells by Ki67 detection (red) and relative quantification and (F) ratio between hSkMC and hFb (scale bar = 100µm).

The proportion of hSkMC and hFb was monitored during the course of tissue-like construct cultures. Interestingly, despite the number of seeded hFb was the same in each condition, mechanical strain exerted a different stimulus to dynamic cultured samples, helping in some way to keep high the number of myoblasts and controlling the proliferation of fibroblasts which, on the contrary, rapidly increase in static constructs reaching 60% of the total cell number after 14 days (Fig. 4.7 A). In line with this finding, dynamic samples presented in a stronger manner, specific proteins of the skeletal muscle compartment and functionality, such as MHC and ACTA (Fig. 4.7 C, D), whereas the expression of myogenic marker MYOG was the same in both conditions (Fig. 4.7 B).

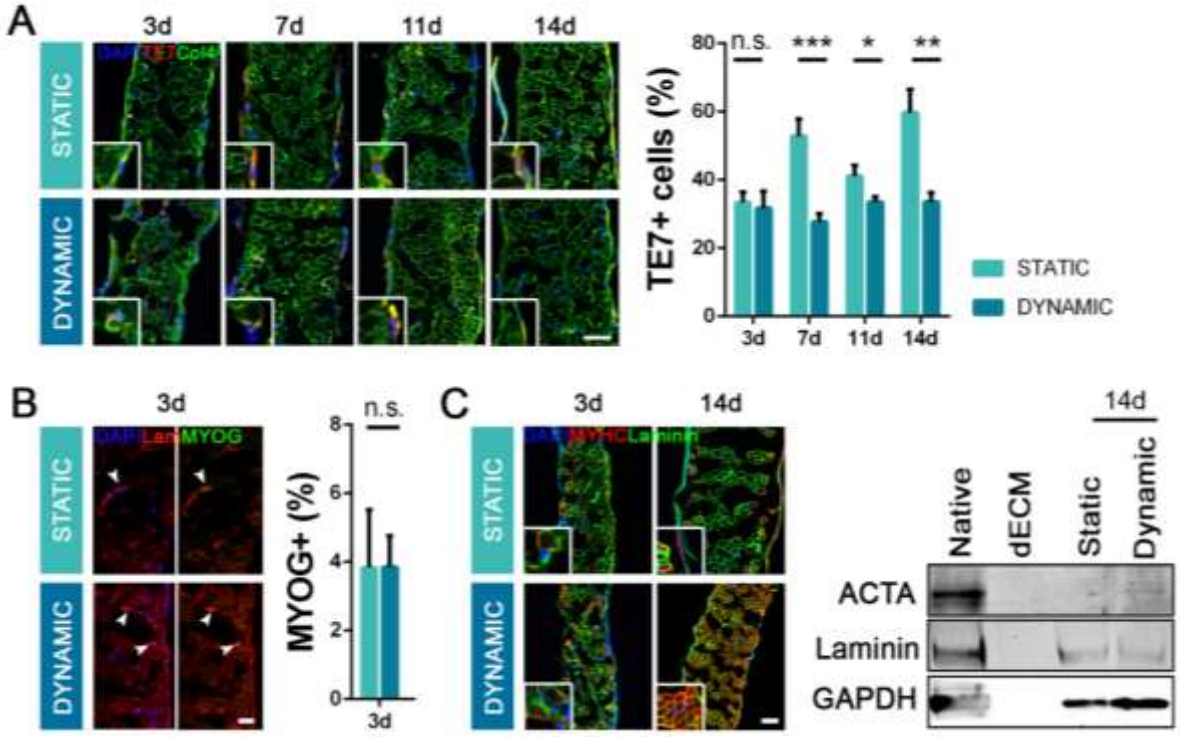

Fig. 4.7. Dynamic vs Static Bioreactor culture myogenic characterization

(A) Immunofluorescence analysis of hFb positive cells for Te7 marker (red) and relative quantification during the culture condition, Col4 marked in green. (B) Immunofluorescence of Myogenin (green) expression and relative quantification at 3 days, (C) MYHC expression (red) at early (3 days) and late time point (14 days). (D) Western blot analysis of static and dynamic construct and relative controls (scale bar = 100μm).

4.3 Engineered pathological diaphragm-like tissue construction

4.3.1 Immortalized human healthy myoblast

Primary myoblasts can be isolated from patients but are rare and precious, their replicative rate is limited and during expansion primary myoblast lose their differentiation potential. In addition, the cell number availability is a limitation for tissue engineering application. For this reason, we planned to use immortalized myoblasts prepared from patients' primary cultures. Immortalization is accomplished by lentiviral transduction of primary cells with the murine cyclin-dependent kinase (cdk)-4 and of human telomerase reverse transcriptase (hTERT) [93]. Transduced myogenic cells are expected to possess a much longer lifespan without changing their myogenic potential.

We hold aliquots of myogenic cells from healthy patient thanks to the collaboration with Professor Doriana Sandonà of Biomedical Sciences Department, University of Padua. We tested immortalized myogenic cells to recellularize healthy or pathological dECM in order to obtain a patient derived construct as proof of principal of advance personalized modelling in vitro. First, we characterized the immortalized healthy myogenic cell line, named AB678, alone and mixed with hFb (85% AB678, 15% hFb) in 2D standard culture condition. AB678 are characterized by a good proliferation rate during first days of culture in proliferating condition; when switched in differentiation medium, cells are able to differentiate and express late myogenic markers such as αSG and MYHC (Fig. 4.8 A). In the mixed population it is appreciable the expression of Col4, produced by TE7+ hFb in the differentiated culture (Fig. 4.8 B).

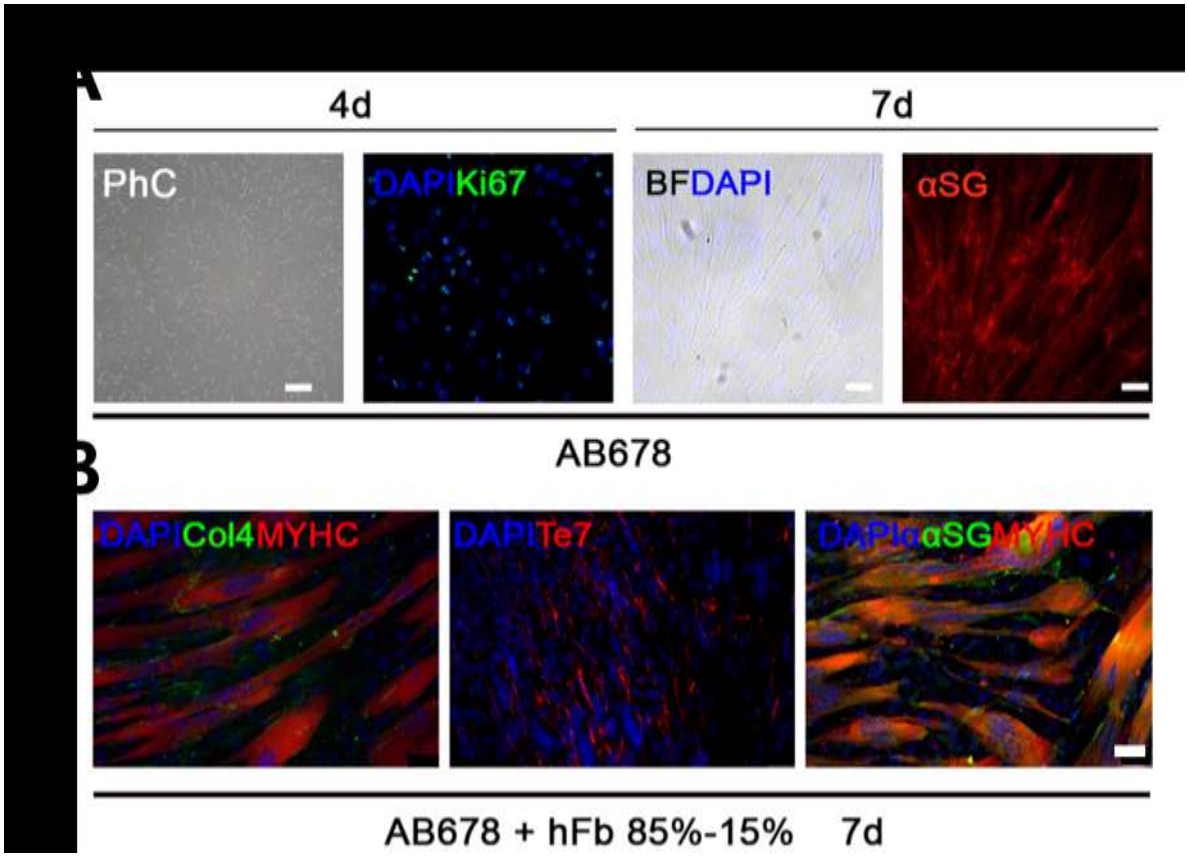

Fig. 4.8 Characterization of healthy immortalized myogenic cells

(A) phase contrast and Immunofluorescence images of AB678 cells in proliferating (4d) and differentiation medium (7d), Ki67 proliferating positive cells are shown in green, αSG expression in red. (B) Co-culture AB678 (85%) and hFb (15%) at 7 days after differentiation (scale bar = 50 μm).

We performed preliminary experiments in a static setting until day 7, to test the repopulation and differentiation ability of AB678 cells within αSG KO dECM, in order to evaluate and compare the cell myogenic ability within the complex 3D scaffold with the 2D standard culture condition. In Figure 4.9, it is interesting to note that myogenic cells were able to engraft and repopulate the αSG defective matrix, as proven by the presence of DAPI signal (nuclei) throughout the scaffolds, appreciable from the sagittal point of view, confirming that cells are present all over the dECM, but also by the transversal cutting sections of the construct. Engrafted healthy cells maintained the differentiation capacity; indeed, they expressed α- and β-SG as shown by WB analysis that is absent in the dECM alone. The protein lysates from native αSG null and healthy wild type muscles were used as positive and negative control, respectively.

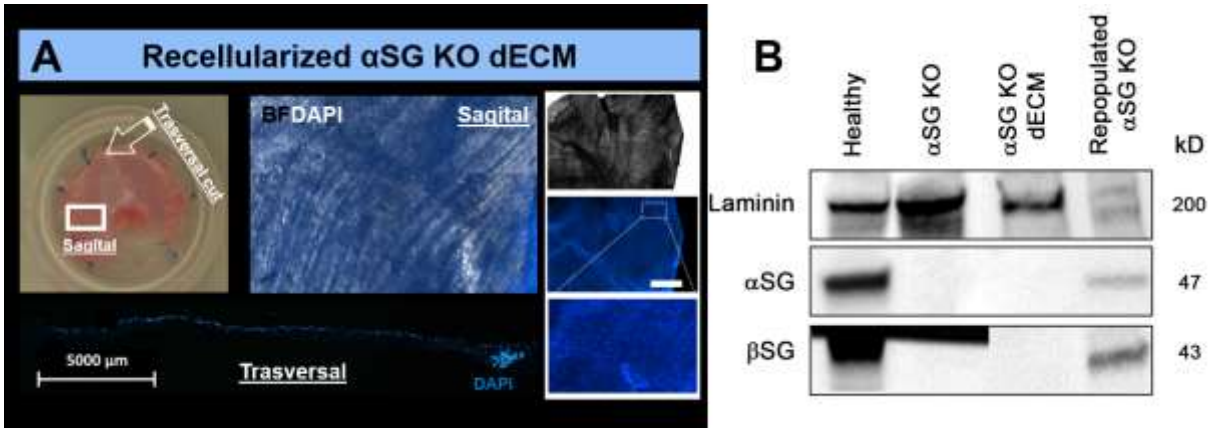

Fig. 4.9 Recellularized αSG KO dECM with immortalized myogenic cells.

(A) Recellularization evaluation by whole mounting immunofluorescence and bright field of nuclei within dECM (scale bar = 100 µm). (B) Western blot analysis of recellularized αSG dECM and relative controls.

4.3.2 Pathological diaphragm-like construct characterization

Then we perform recellularization experiment based on our previous results of dynamic bioreactor culture. Instead of hSkMC we used AB678 to obtain the mixed population to inject in parallel within the healthy or αSG KO dECM. The constructs were culture until day 7 in static or dynamic condition following our previously defined protocols. We evaluated cell engraftment, distribution and interaction with the dECM. By immunofluorescence analysis we found that the main difference between the constructs is the presence of αSG protein only in the healthy scaffold, whereas other ECM component (Col1, Col4, Lamininα2) are preserved in both dECM types. The cells were able to engraft and repopulate both the scaffolds but seemed to interact better with the healthy dECM, where the cells express more F-Actin protein, especially in the dynamic condition (Fig. 4.10 A). This data of better crosstalk with the scaffold is also supported by cell distribution analysis. Dynamic stimulation seems to be more favorable in the healthy construct to influence cell distribution throughout the scaffold, and a statistically significant percentage of cells was found in the lower construct side (46.6±4.1%) in comparison with static culture (34.9±9.1%). Instead, not significant difference between static and dynamic conditions was found when the αSG KO dECM is used (Fig. 4.10 B, C).

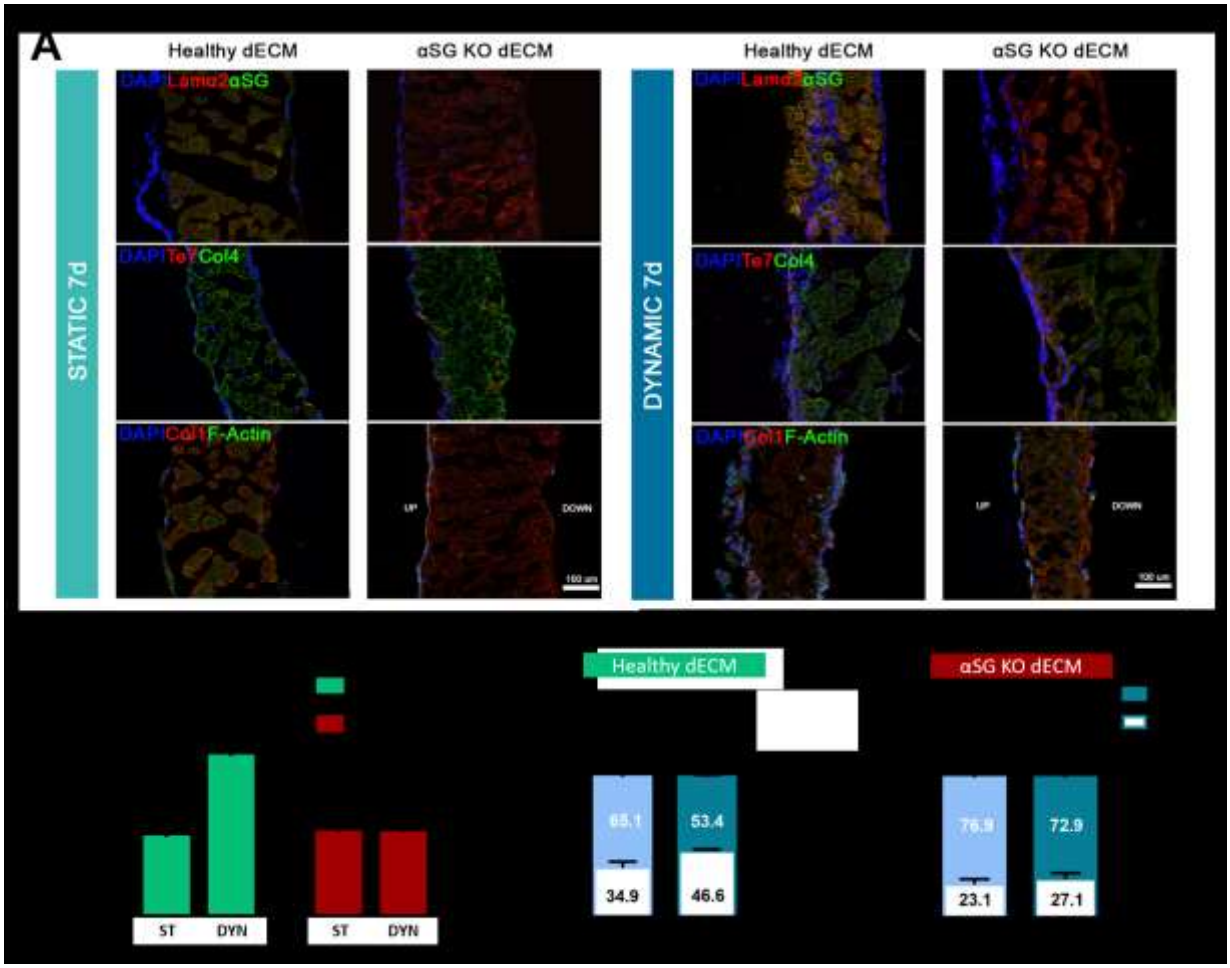

Fig. 4.10 Recellularized healthy and αSG KO dECM in static and dynamic bioreactor culture. *(A) Immunofluorescence analysis of healthy and αSG KO dECM recellularized in static or dynamic bioreactor at 7 days. (B) Cells distribution among area and (C) in the upper (UP) or lower (DOWN) side of the dECM (scale bar = 100μm).*

4.4 Pig dECM and clinical translation for CDH treatment

4.4.1 Perfusion decellularization of piglet diaphragm

With the aim of making a step towards the clinic, we focused our attention on diaphragm sources that could be useful in a possible CDH treatment application. For this reason, we set-up a decellularization protocol for piglet diaphragms using a perfusion method that allowed us to exploit the muscle vascular tree to completely remove cells and to preserve tissue ECM composition (Figure 4.11 A). Piglet has weight and size comparable to newborns, so we evaluate

a decellularization strategy to obtain an entire decellularized organ that resemble the clinical reality dimension needed. Native diaphragm was collected from healthy piglet (weight 3Kg) and then taking advantage of natural vascular access, we cannulated the inferior vena cava (IVC) and perfused the solutions to obtain the organ decellularization. As we previously showed for mouse dECM, we verified that after 3 detergent enzymatic treatments, a complete cell removal was achieved (Fig. 4.11 A). Moreover, primary ECM components, such as collagens were maintained, as well the preservation of the complex architecture and ECM organization as underlined by histological images and collagen quantification, only sGAG quantification showed aa significant decrease after decellularization (Fig. 4.11 B).

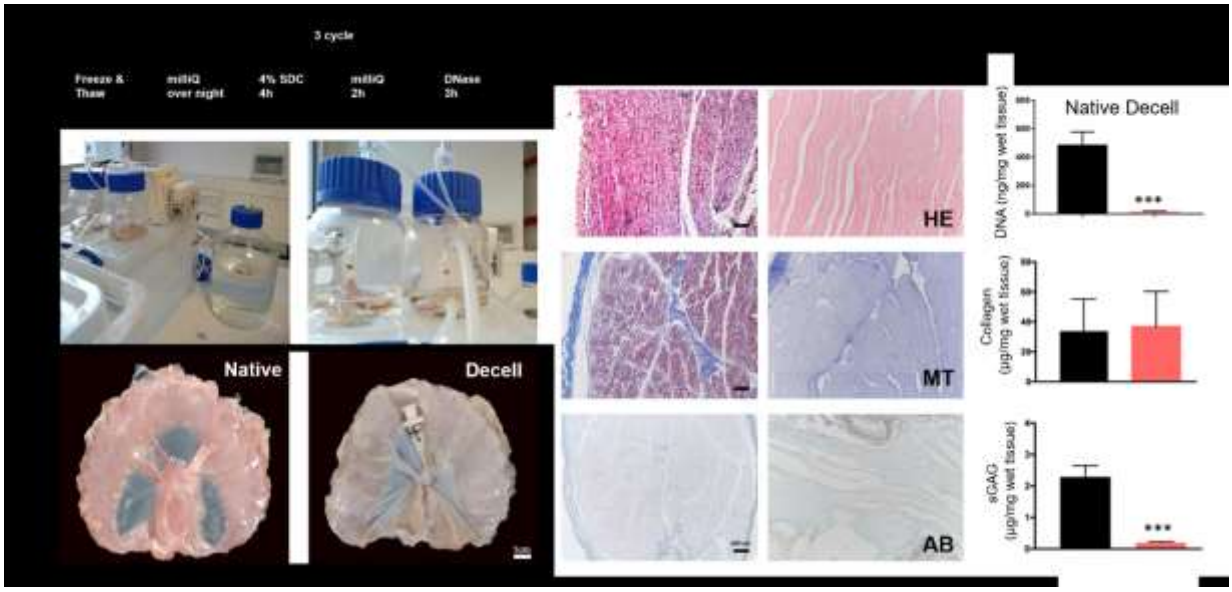

Fig. 4.11 Decellularization through perfusion system. *(A) In home developed system for perfusion decellularization ensuring sterility and reproducibility trough peristaltic pump and sterilized bottles. Comparison between native and decellularized (Decell) piglet diaphragms (scale bar = 1 cm). (B) Staining and quantification of ECM components before (Native) and after decellularization by histological staining: Hematoxylin & Eosin (HE), Masson's Trichrome (MT) and Alcian Blue (AB) (scale bar = 100 µm) and collagens and sGAG quantification.*

4.4.2 Diffusion decellularization of porcine diaphragm

With the idea to be able to standardize and characterize a well define product from the beginning of the protocol, we explore another decellularization strategy to obtain clinically relevant dECM product for CDH treatment. We choose to perform decellularization by diffusion and agitation

in alternative to perfusion of the entire organ, trying to optimize the decellularization protocol. Decellularization by diffusion is more easily to perform because does not requested the surgical harvesting of intact diaphragm with preserved IVC. Moreover, the native tissue can be stored before decellularization without concern for the vascular tree preservation that is needed integral to perform an efficient perfusion decellularization. We standardized the source of tissue collection from sacrificed healthy porcine animal (25 kg) for the food market; then, after collection, native diaphragm muscles were stored at -80°C until decellularization. After defrost process and before decellularization, the native diaphragm was dissected in patches of defined size: 3 x 4 cm, with a mean natural thickness of 0.5 cm (Fig. 4.12 A). The epimysium was dissected from diagrammatic muscle, only a portion of the central tendon was maintained as useful surgical stitch area. Native ECM patches were decellularized with 4 DET cycles by agitation/diffusion. Immunofluorescence of specific ECM components Col1, Col4, Actin, underlined the preservation of native ECM architecture and composition as well as the cell removal, also confirmed by DNA quantification (Fig. 4.12 A, B).

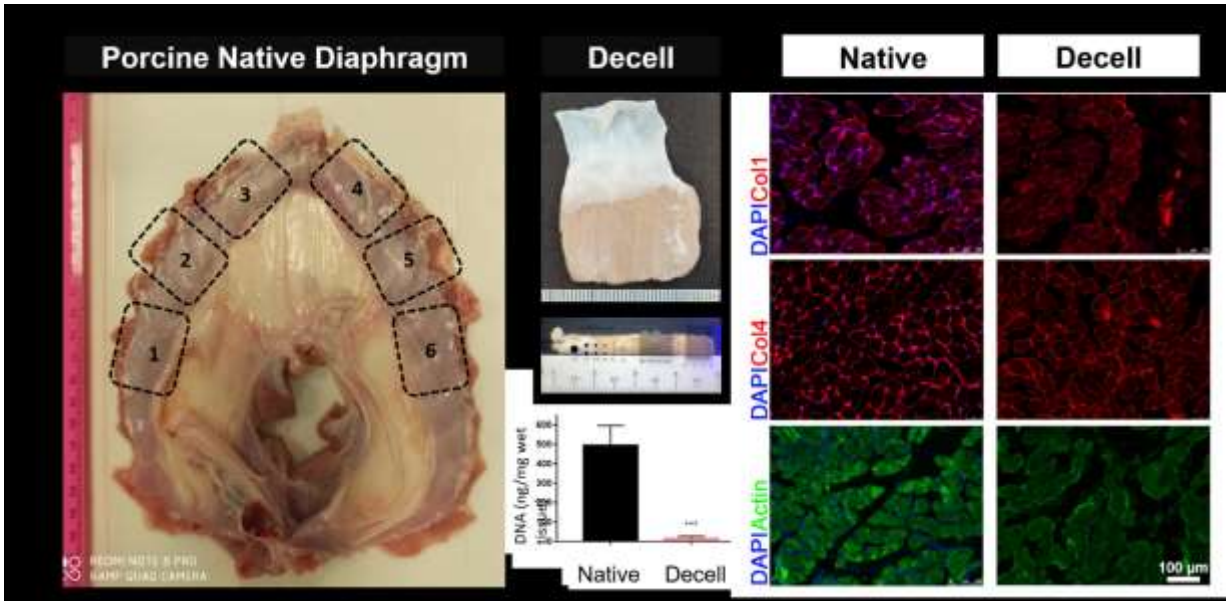

Fig. 4.12 Decellularization through diffusion & agitation. *(A) Macroscopic view of native porcine diaphragm and derived Decell patch. (B) Immunofluorescence of native and decell porcine diaphragm for Col1, Col4 (red) and muscle actin (green), nuclei counterstained with DAPI (scale bar = 100µm).*

Moreover, SEM and TEM analyses (Fig. 4.13 A) confirmed the decellularization efficiency, nuclei depletion and highlighted the retention of ultrastructural integrity of the main skeletal

muscle units, such as the striated pattern of retained myofibrils inside parallel and well organized myotubes “ghost fibers” grouped into fascicles.

Native and dECM patches were subjected to tensile tests, performed in the Planar Biaxial TestBench Bose® Electro-Force. Stress-strain data shown that after the decellularization process the dECM maintained values comparable with the native tissue; this point is crucial in order to consider dECM patch a reliable material for human application in vivo on newborns, where the tension and the mechanical strains are strong (Fig. 4.13 B).

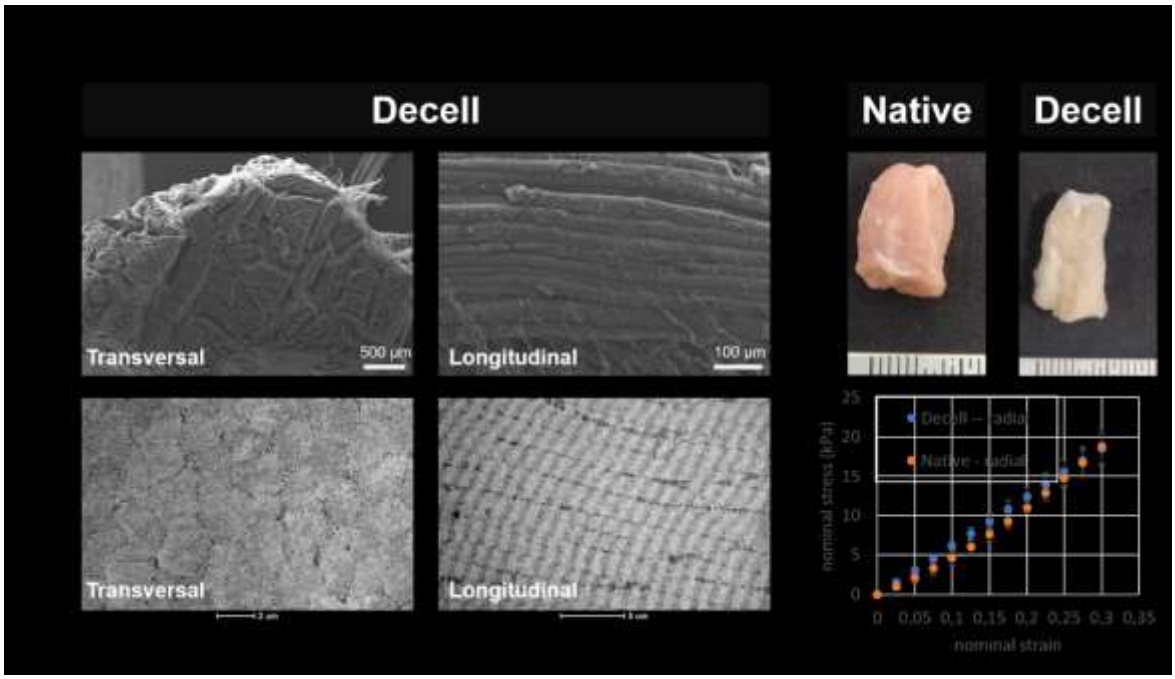

Fig. 4.13 Biomechanical and structural characterization of dECM patch. *(A) SEM and TEM transversal and longitudinal section of dECM patch. (B) Macroscopic view of native and dECM samples used to test the mechanical properties and nominal stress vs strain.*

The Food and Drug Administration (FDA) regulates biologic scaffolds derived from xenogeneic source tissue, including material derived from decellularized porcine tissues, as medical devices, therefore requiring these products to be terminally sterilized prior to clinical use. Common methods of terminal sterilization include electron beam (e-beam), gamma irradiation and ethylene oxide. It is known that each of the before mentioned methods exerts its sterilizing effect by modifying the structure or function of the critical components (e.g. proteins) of target microorganisms and has directed guidelines regarding bacterial load. For this reason, we performed preliminary experiments of dECM terminal sterilization by using γ -irradiation, and alternatively, the incubation with PAA, used also by others for the sterilization of decellularized

tissues. dECM derived from perfusion decellularization were sterilized using γ -irradiation, whereas dECM patch obtained from agitation diffusion were treated with PAA, as illustrated in 3.13 and 3.14 sections. As shown by graphics in figure 4.14 both treatments allowed to efficiently sterilize the dECM.

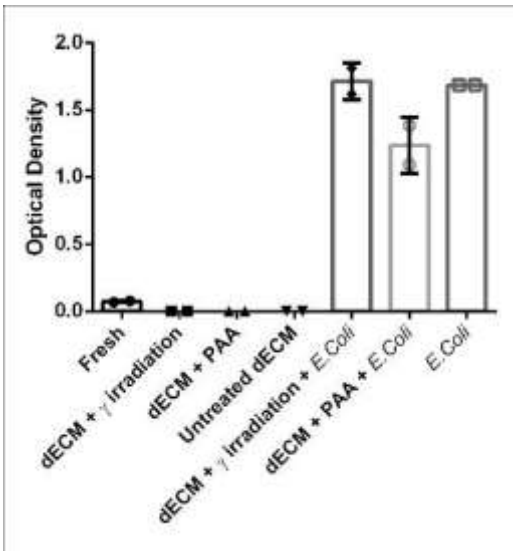

Figure 4.14 Preliminary results of LB culture with different samples of terminally sterilized and non-sterilized dECM samples. *Fresh: native diaphragm without sterilization treatment. dECM + γ irradiation: dECM sterilized with γ irradiation. dECM + PAA: dECM treated with 1.5% PAA for 3h. Untreated dECM: decellularized sample without sterilization treatment. E. Coli: positive control analyzed alone or in combination with sterilized samples.*

With the aim of deeply analyzing the bioactive properties of porcine diaphragm dECM and testing *in vitro* the ability of this type of scaffold to sustain cell engraftment and proliferation, we carried out preliminary experiments of recellularization using hSkMC and relevant dECM patch (1x0.5x0.5 cm). After decellularization process, dECM patches were lyophilized and store at – 20°C, as proof of concept of an "off the shelf" and ready to use biocompatible material. Then, prior to recellularization, lyophilized dECM were thaw at room temperature and a mixed population (cell density: 4 x 10^6) of hSkMC (85%) and hFb (15%) was injected directly within the scaffold with an insulin syringe (30G). We used 150 µL of the same combination of factor to resuspend and vehicle the cells within the lyophilized dECM in order to re-hydrated completely the scaffold area. The constructs were cultivated in 24 well culture dish with 2 mL of proliferating medium until day 4 to switch then to the differentiation medium until day 7. The cells were able not only to engraft and proliferate inside the scaffold, but also to express and

secrete important adhesion molecules (i.e. F-Actin, Laminin) composing the natural muscle ECM environment (Fig. 4.15), confirming the idea that porcine diaphragm dECM may be a suitable material for CDH treatment.

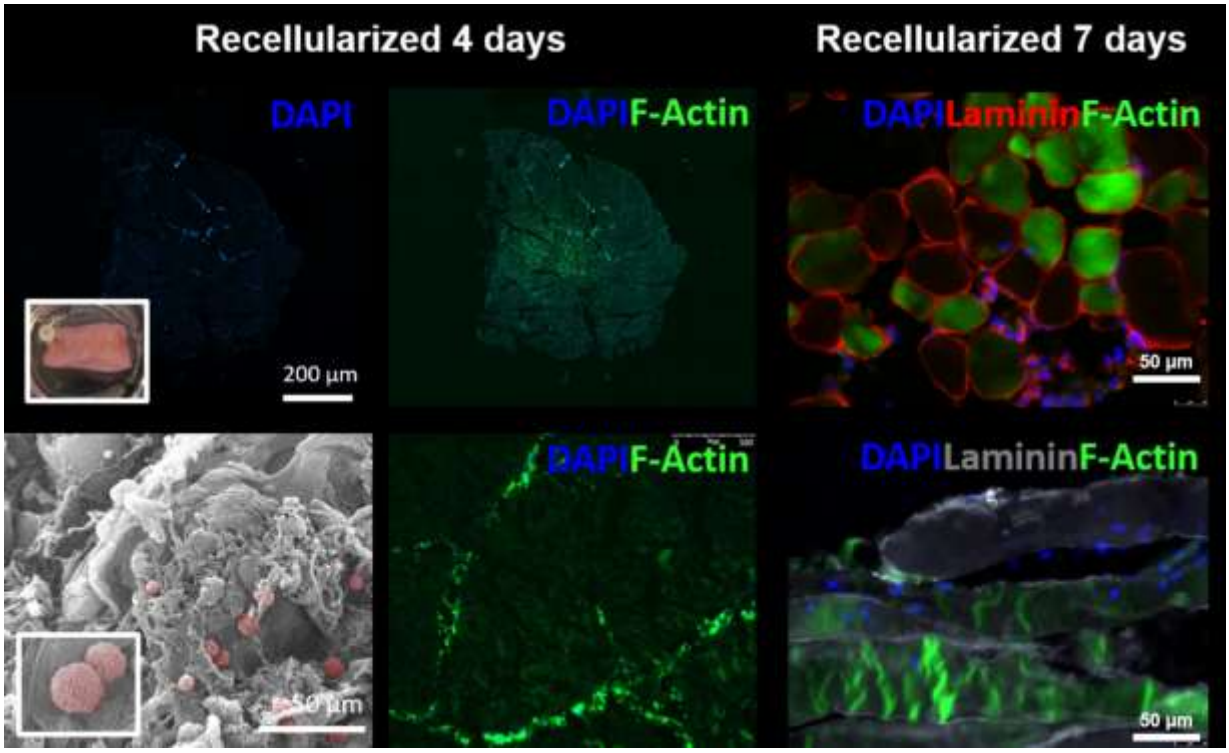

Figure 4.15 Preliminary recellularization experiment of porcine dECM. *Immunofluorescence cross sectional area section of relevant size dECM recellularized construct and SEM analysis to evaluate engraftment and interaction at 4 days. Immunofluorescence at day 7 shown transversal and longitudinal F-actin and Laminin interaction with cells counterstained with DAPI (scale bar = 50µm).*

5. Discussion

Engineering skeletal muscle in vitro for advanced patient-specific therapy remains a challenge. Even if tissue engineering approaches are becoming a reality, protocols optimization and GMP pipelines standardization to obtain advance personalized models are not still available and reliable. Different strategies are pursuit in order to recreate native cues and stimuli that mimic the in vivo muscle tissue environment, chasing the complexity to properly recapitulate the correct network of cell interactions, scaffold environment and bioreactor stimulation strategies [94]. The fundamental role that ECM plays not only as structural component but also as cardinal regulator of development, homeostasis and repair, that ultimately ensure the proper functionality of skeletal muscle tissue are becoming everyday more important and relevant as disclosure by different studies and approaches [95-99]. Recently we characterized the ECM obtained from decellularized healthy mouse diaphragm. Healthy dECM possesses structural, biochemical and biomechanical characteristics similar to those of the fresh native tissue [88]. dECM also demonstrated to be a suitable scaffold for the proliferation and differentiation of human muscle precursor cells (hMPCs) from pediatric patients, allowing the generation of a 3D skeletal muscle construct containing both muscle stem cells and differentiated myotubes, as proof of principle for future preclinical and clinical studies [90]. In general, the need to improve our knowledge of the relationships between cells and ECM both in healthy and diseased environment it is becoming more pressing. In the pathological condition, the clinical need to ameliorate disease managing and pharmacological treatment in an ever more specific way has become a very flourishing field of study, especially in the oncological research [100, 101]. Several works demonstrated that decellularization allows to obtain tissue specific scaffolds preserving the original features of native tissue, even from patient biopsies of primary tumor and metastasis [102-104]. Developing real 3D constructs directly from patients' tissue samples that closely mimic the phenotypical and biological properties of the cancer microenvironment, could be useful to dissect pathological mechanisms and elucidate pivotal interactions between cell and its environment, opening new specific and targeted therapeutic treatments. Here, we explore and consolidate the efficiency of our decellularization method to preserve ECM architecture and biochemical composition of the original native tissue, comparing healthy and pathological diaphragmatic ECM components. In this context, pathological dECM can be used as new scaffold that more realistically reproduces ECM skeletal muscle disease and phenotype than 2D

culture models, providing stimuli (e.g., soluble factors and physical strain) that strongly influence cell functions and gene expression profile. In sarcoglycanopathies, the absence of a key component of the dystrophin-associated protein complex renders muscle cells susceptible to stretch-induced damage and fiber necrosis, even if the complete sequence of events is not fully disclosed. SGs are glycosylated transmembrane proteins; their biosynthesis occurs into the endoplasmic reticulum where they undergo folding, glycosylation and assembly into the tetrameric complex that moves toward the sarcolemma. At the sarcolemma, SG-complex becomes part of the dystrophin-associated complex playing a major role in membrane stabilization. Therefore, from a phenotypic point of view, sarcoglycanopathies manifest with the absence of ECM proteins that surround muscle fibers and are fundamental for the stabilization of muscle contraction. Healthy and αSG KO diaphragm muscles were decellularized and compared, highlighting once again the preservation of specific native ECM proteins, that showed the αSG expression in the basal lamina of healthy muscle fibers versus the absence of the protein in the αSG KO model that confirmed the pathological ECM dysregulation. Moreover, the architectural integrity of the whole diaphragmatic anatomy was confirmed by ECM component organization that mirrors the proper anatomical location of Col1, Col4, Lamininα2 between muscle fibers and residual muscle actin inside each myofiber.

We previously reported the production in vitro of a viable and functional construct combining healthy dECM and hMPC in static culture condition [90]. We showed that diaphragm-like tissue maintained not only a heterogeneous pool of myogenic cells, but also responded to external stimuli. Indeed, after chemical injury, the construct regenerated by activating the stem cell pool and producing new muscle fibers. Predictably, the newly generated myofibers randomly aligned, due to the absence of specific directional stimulation inside the tissue culture, affecting the contraction ability of the muscle construct. One of the major limits of that work, in fact, was the absence of external stimuli that recapitulate the dynamic mechanical load typical of skeletal muscle tissue, very significant in the case of diaphragm muscle that exerts his function all over our life-span. Differently from other human muscles, diaphragm presents a unique anatomy of a flat shape, with a central tendon and outward radiating myofibers. With the notion that mechanotransduction plays a central role in myogenic differentiation, mechanical stimulation has been demonstrated to induce cellular alignment along the axis of strain [105-109] and to stimulate muscle growth in vitro and in vivo. Taking advantage from this central concept, here

we scaled up and developed a specific and unique dynamic bioreactor system for diaphragm-like tissue constructs, designed according to its anatomical conformation, geometry and function by FEM modelling based on mouse physiological data. Up to now, bioreactor system for skeletal muscle engineering are developed and produced with the final aim of linear muscle production, following a single axis of strain and orientation, which in some cases leads, after the 3D construct maturation, to a single axis of contraction. Here, the complex and unique anatomy of diaphragm, with myofiber organized in a radial disposition leads us to design and fabricat for the first time a diaphragm-specific bioreactor. The ability to control cell disposition, alignment and maturation *in vitro* within a standardized, validated and optimized bioreactor system, able to perform multiple experiment with tunable stimulations, is certainly one of the most important aspects of our approach in order to consolidate the bioreactor as a fundamental tool for tissue engineering purposes. Following literature findings [113-116], we choose to investigate and apply two different types of radial strain to our diaphragmatic constructs: (1) a slow stress ramp strain that aimed to replicate the progressive and continuous stress that occurs by bone elongation during muscle embryogenesis, in order to induce cell engraftment, orientation, direction and spreading within and around the dECM ghost myofibers; (2) a training protocol in order to replicate the muscle cyclic elongation movement that occurs during exercise and homeostasis in adulthood.

To recellularized an entire diaphragm dECM, we choose to inject 3 million of cells that seems to be a good compromise considering our previous protocol [90], where we used 500.000 cells to recellularized approximately 35 mm^2 of patch dECM. Furthermore, we used a mixed population of commercially available primary cell lines rather than primary human MPCs because more feasible and repeatable, allowing the reproducibility of data to ensure the standardization of the mechanical loading protocols. We characterized the two cell lines for the expression of specific markers in order to easily individuate behavioral changes that occurs during the culture in the different settings. Specifically, we evaluated the myogenic potential of hSkMC by analyzing myogenic master regulator factors, such as MYOD, MYOG and by calculating myogenic index; in parallel we identified hFb for Te7 and αSMA specific expression. After cell injection, we take advantage of glucose real-time biosensors to monitor cell consumption during the culture, allowing the real-time monitoring of cell viability and starvation, parameters than often can be underestimated in tissue engineering modelling but that have real impact on cell behavior and successful experimentation. Indeed, we observed a similar

consumption pattern on both conditions (dynamic vs static) in the majority of the performed experiments, but the sensor allowed us to rapidly identify samples that for some experimental reasons did not have proliferating cells and were in fact not recellularized, helping us to save time and valuable material. Glucose consumption data suggest that in our setting cell metabolism is very rapid and each other day was needed a glucose addition in order to avoid cell starvation that can be on the contrary finely monitored when activation of specific metabolic pathways should be forced within the construct. In the dynamic setting the applied mechanical stimulation better distributed the injected cells in both scaffold sides with a percentage of cells in the lower side that is almost double in the dynamic setting in respect to the static culture. This data suggests a positive effect of the initial slow ramp stimulation applied to the construct that seems to positively influenced cell spreading inside the dECM, confirming the importance of mechanical strain in the generation and maturation of engineered skeletal muscle. Indeed, dynamic cultured constructs demonstrated to express in a stronger manner functional muscle proteins respect to static samples that on the contrary presented an increased proliferation of hFb. This opposite effect is in line with the literature findings, in which mechanical strain was demonstrated to induce a precise myoblast alignment and fusion into myotubes [110], but also to arrest fibroblast proliferation and induce their apoptosis [111, 112].

Analyzing the pathological ECM setting, all the applied stimuli and environment conditions exerted a change in the seeded cell behavior. Differently from healthy scaffolds, α–SG KO dECM arrested or at least reduced cell spreading that resulted very similar between static and dynamic samples, abolishing in some way the positive effect obtained with mechanical strain in the healthy constructs. Since the differences between healthy and α–SG KO dECM is exclusively the absence of α–SG and the related dystrophin-associated proteins, it is reasonable to suppose that the lack of structural ECM proteins could alter cell engraftment and distribution, pushing us to investigate in more detail the role of this protein on cellular behavior and even more in skeletal muscle homeostasis. More experiments are needed to validate this experimental setting, analyzing longer time point and the effect of different mechanical loading, but in a clinical perspective, the 3D α–SG KO diaphragmatic construct could be consider a good pathological model to investigate the mechanisms underpinning this devastating muscle disease.

With the aim to validate and translate our tissue engineering approach based on dECM stand alone as new biomaterial suitable for CDH clinical application, we scaled up and explored the possibility to obtain diaphragm dECM from porcine donors. As mentioned before, for large CDH defects in pediatric patients, the current treatment is the use of prosthetic patches to close the malformation, but these materials do not evolve with the child growth, leading to frequent hernia recurrences and co-morbidities. Several non-tissue specific acellular matrices were used to repair CDH (i.e. Alloderm®, Pericardial tissue, SurgAssist®), and despite their biocompatibility and efficiency when used in other organs, the overall results in terms of drawbacks and hernia recurrences, were poorer than those of standard Gore-Tex patch treatment[30, 31, 35]. Given the current suboptimal repair methods, we recently showed, for the first time in the literature, the superiority of diaphragm dECM for the closure of a diaphragmatic defect in a new surgical murine model of diaphragmatic hernia [113]. Despite the advantages of using small animal models in transplantation, a plethora of data confirm that experiments in rodents are not sufficiently relevant to predict human responsiveness to potential treatment strategies. To confirm and validate this results the development of a large animal model to be used as essential pre-clinical test for validating the efficacy and safety of dECM implantation is a necessary step. Here we consider piglet as the ideal diaphragm donor source to translate our approach in order to verify the efficiency of our decellularization method to produce tissue specific dECM as new treatment option for large CDH defects. Young porcine diaphragm dimensions and thickness are very similar to those of newborn, thereby making analyses and read outs compatible with the needs of little patients. We set-up a decellularization protocol for porcine diaphragms using a perfusion method that allowed us to exploit the muscle vascular tree to completely remove cells and to preserve ECM architecture and composition. We evaluated different strategies to perfuse the whole diaphragmatic muscle, exploring aorta and thoracic arteria cannulation, where the major limit was the anatomical necessity to preserve the rib cage during the decellularization process in order to maintain intact the main vessels. Unfortunately, this procedure led to frequent sample contamination vinifying the effort to pursuit this option. On the contrary, the IVC cannulation seems to be a more suitable and reasonable solution, indeed the excision of the entire diaphragm muscle from the rib cage allowed us to perform the decellularization protocol under more reliable conditions, inside a specific developed system to ensure reproducibility and sterility. We verified that after 3 DET cycles by perfusion, a complete cell removal was achieved together with ECM component preservation as shown by histological analysis and collagens and

sGAG quantification. Nevertheless, decellularization by perfusion is limited by surgical compliance when IVC or other vessels are not well preserved or disrupted. These technical impediments can lead to leaks during the reagent perfusion and therefore to an un-efficient or partial decellularization all over the muscle diaphragm. FDA regulates biologic scaffolds derived from xenogeneic source tissues (e.g. decellularized porcine tissues) such as medical devices; therefore, these products require to satisfy precise and mandatory aspects such as the standardization of the pipelines production of the device, which must follow GMP guidelines, starting from the definition of the healthy state of the donor source to the final need of efficient terminal sterilization step prior to clinical use. In this contest, to deepen the possibility to fabricate an advanced therapy medicinal product that fit all these parameters, we decide to adopt and verify an alternative strategy to produce relevant acellular dECM patches. We choose to perform decellularization by diffusion and agitation of define weight and size of dECM patches in alternative to perfusion of the entire organ, trying to optimize stringent parameters of the decellularization protocol. Decellularization by diffusion is more easily to perform because does not request the surgical harvesting of intact diaphragm with preserved vessels. This approach allows us to standardize and validate a suitable protocol that follow GMP guidelines, from the source of tissue collection (healthy porcine from veterinary checked animals for food market), to decellularization efficiency, from mechanical properties to final evaluation of terminal sterilization methods. To achieve a proper decellularization efficiency we used 4 DET cycles that confirmed DNA removal and ECM component preservation as showed by immunofluorescence analysis of collagens (Col1, Col4) and also specific residuals of myofibrillar component such as muscle actin. As underline by SEM and TEM analyses, the micro and macro myotubes organization within myofiber fascicles and bundles is perfectly maintained after decellularization. Notably, the retention of the hallmark of skeletal muscle tissue, the characteristic Z-band pattern, is also appreciable by TEM sections, confirming the absolute potential to maintain almost unalerted the overall tissue conformation and ultrastructure. As mentioned before, a crucial aspect to define a decellularized patch suitable for transplant proposals is the terminal sterilization step. We choose to investigate two of the most adopted methods in the literature: γ-irradiation and PAA treatment. Preliminary data of bacterial contamination assays confirmed that both methods allowed to efficiently sterilize the porcine derived dECM. However, to find the ideal sterilization treatment, further investigation on structural changes/modifications of the scaffold due to the aggressive action of these techniques

is needed. Then we analyzed the mechanical properties of dECM in order to evaluate the possibility to apply these patches in vivo, where we must consider the enormous strain to which dECM will be undergo in the clinical scenario. The data suggest that even after the decellularization, the mechanical properties remain comparable with those of the native tissue and computational methods should be adopted to design the setup for the mechanical stimulation, following an approach already applied successfully in previous experiences in the mouse model. Another important step that we analyzed was the definition of lyophilization step as final methods to preserved terminal sterilized dECM until in vivo or vitro application. Despite we previously demonstrated that murine dECM could be stored for long period in liquid nitrogen following all the procedures classically adopted for cell storage [90], a simpler and cheaper method should be standardized for clinically relevant dECM patches, to facilitate the production chain. Finally, we tested the biocompatibility of porcine dECM by recellularization procedures, with the final aim to verify the acceptance property of the scaffold and the ability to sustain cell engraftment and survival when implanted in vivo. We scale up our pervious protocols for mixed cell injection, validating the idea to re-hydrated lyophilized dECM with proper growth factors and cells. This indeed is a possible and feasible solution to scale up and translate our tissue engineering approach to finally use this scaffold for personalized advance therapy. Cells were able to engraft and interact with the matrix as showed by immunofluorescence analysis, indicating a good interaction between cells and porcine scaffolds. To test the porcine dECM ability to integrate with recipient diaphragmatic muscle and to withstand to in vivo mechanical strain, further in vivo experiments are needed.

6. Conclusion

In the present work, we established a reliable decellularization protocol in order to obtain pathological dECM as new option to model in a more realistic way realistic a native microenvironment.

We developed a specific bioreactor system, specific designed for engineered diaphragm-like constructs, in which the mechanical stimulation boosts cell engraftment, interaction and maturation within the dECM scaffold. The dynamic culture influences hSkMC and hFb crosstalk in a positive manner mirroring cellular behavior observed in vivo.

We showed the possibility to obtain pathological diaphragm-like tissue that recapitulate the main critical aspect of the muscular disease. These preliminary data suggest that dECM composition plays a role during recellularization process, indeed the positive outcomes influence observed after dynamic culture in healthy dECM are partially reduced when pathological dECM are use. This aspect should be studied and investigate more in details but suggests the possibility to recreate in vitro an advance personalized 3D model that can recapitulate specific phenotypic features.

We demonstrated the possibility to obtain clinically relevant acellular dECM from porcine source, showing the versatility and transability of our decellularization protocol. We showed the production of dECM in which the main mechanical and biological features as comparable with the native tissue and verified some crucial aspect that have to be keep in mind, such as terminal sterilization and bio-acceptance, to translate the product into the clinical practice.

We believe that this work represents a step forward toward the generation of advance personalized diaphragmatic-like muscle in vitro model and tissue specific diaphragmatic acellular patch for skeletal muscle clinical applications in large CDH repair.

Bibliography

1. Lieber, R.L., *Skeletal muscle architecture: implications for muscle function and surgical tendon transfer.* J Hand Ther, 1993. **6**(2): p. 105-13.

2. Mauro, A., *Satellite cell of skeletal muscle fibers.* J Biophys Biochem Cytol, 1961. **9**: p. 493-5.

3. Chang, N.C. and M.A. Rudnicki, *Satellite cells: the architects of skeletal muscle.* Curr Top Dev Biol, 2014. **107**: p. 161-81.

4. Zammit, P.S., et al., *Pax7 and myogenic progression in skeletal muscle satellite cells.* J Cell Sci, 2006. **119**(Pt 9): p. 1824-32.

5. Baghdadi, M.B. and S. Tajbakhsh, *Regulation and phylogeny of skeletal muscle regeneration.* Dev Biol, 2018. **433**(2): p. 200-209.

6. Evano, B., et al., *Dynamics of Asymmetric and Symmetric Divisions of Muscle Stem Cells In Vivo and on Artificial Niches.* Cell Rep, 2020. **30**(10): p. 3195-3206 e7.

7. Bentzinger, C.F., J. von Maltzahn, and M.A. Rudnicki, *Extrinsic regulation of satellite cell specification.* Stem Cell Res Ther, 2010. **1**(3): p. 27.

8. Andrade, W. and E. Brandan, *Isolation and characterization of rat skeletal muscle proteoglycan decorin and comparison with the human fibroblast decorin.* Comp Biochem Physiol B, 1991. **100**(3): p. 565-70.

9. Lipton, B.H. and E. Schultz, *Developmental fate of skeletal muscle satellite cells.* Science, 1979. **205**(4412): p. 1292-4.

10. Ahmad, K., et al., *Cross-Talk Between Extracellular Matrix and Skeletal Muscle: Implications for Myopathies.* Front Pharmacol, 2020. **11**: p. 142.

11. Smith, L.R., et al., *Contribution of extracellular matrix components to the stiffness of skeletal muscle contractures in patients with cerebral palsy.* Connect Tissue Res, 2019: p. 1-12.

12. Frontera, W.R. and J. Ochala, *Skeletal muscle: a brief review of structure and function.* Calcif Tissue Int, 2015. **96**(3): p. 183-95.

13. Gao, Q.Q. and E.M. McNally, *The Dystrophin Complex: Structure, Function, and Implications for Therapy.* Compr Physiol, 2015. **5**(3): p. 1223-39.

14. Buckingham, M., et al., *The formation of skeletal muscle: from somite to limb.* J Anat, 2003. **202**(1): p. 59-68.

15. Buckingham, M. and F. Relaix, *PAX3 and PAX7 as upstream regulators of myogenesis.* Semin Cell Dev Biol, 2015. **44**: p. 115-25.

16. Sefton, E.M., M. Gallardo, and G. Kardon, *Developmental origin and morphogenesis of the diaphragm, an essential mammalian muscle.* Dev Biol, 2018. **440**(2): p. 64-73.

17. Merrell, A.J., et al., *Muscle connective tissue controls development of the diaphragm and is a source of congenital diaphragmatic hernias.* Nat Genet, 2015. **47**(5): p. 496-504.

18. Sefton, E.M. and G. Kardon, *Connecting muscle development, birth defects, and evolution: An essential role for muscle connective tissue.* Curr Top Dev Biol, 2019. **132**: p. 137-176.

19. Iozzo, R.V. and M.A. Gubbiotti, *Extracellular matrix: The driving force of mammalian diseases.* Matrix Biol, 2018. **71-72**: p. 1-9.

20. Carmignac, V. and M. Durbeej, *Cell-matrix interactions in muscle disease.* J Pathol, 2012. **226**(2): p. 200-18.

21. Urciuolo, A., et al., *Collagen VI regulates satellite cell self-renewal and muscle regeneration.* Nat Commun, 2013. **4**: p. 1964.

22. Allamand, V., et al., *ColVI myopathies: where do we stand, where do we go?* Skelet Muscle, 2011. **1**: p. 30.

23. Sabatelli, P., et al., *Detecting collagen VI in Bethlem myopathy.* J Biol Chem, 2015. **290**(12): p. 8011.

24. Emery, A.E., *The muscular dystrophies.* Lancet, 2002. **359**(9307): p. 687-95.

25. Guiraud, S., et al., *The Pathogenesis and Therapy of Muscular Dystrophies.* Annu Rev Genomics Hum Genet, 2015. **16**: p. 281-308.

26. Carotti, M., et al., *Repairing folding-defective alpha-sarcoglycan mutants by CFTR correctors, a potential therapy for limb-girdle muscular dystrophy 2D.* Hum Mol Genet, 2018. **27**(6): p. 969-984.

27. Carotti, M., et al., *Combined Use of CFTR Correctors in LGMD2D Myotubes Improves Sarcoglycan Complex Recovery.* Int J Mol Sci, 2020. **21**(5).

28. De Coppi, P. and J. Deprest, *Regenerative medicine solutions in congenital diaphragmatic hernia.* Semin Pediatr Surg, 2017. **26**(3): p. 171-177.

29. Garriboli, M., et al., *More patches or more lung in congenital diaphragmatic hernia?* J Pediatr Surg, 2012. **47**(10): p. 1968-9.

30. Bekdash, B., B. Singh, and K. Lakhoo, *Recurrent late complications following congenital diaphragmatic hernia repair with prosthetic patches: a case series.* J Med Case Rep, 2009. **3**: p. 7237.

31. Grethel, E.J., et al., *Prosthetic patches for congenital diaphragmatic hernia repair: Surgisis vs Gore-Tex.* J Pediatr Surg, 2006. **41**(1): p. 29-33; discussion 29-33.

32. Laituri, C.A., et al., *Outcome of congenital diaphragmatic hernia repair depending on patch type.* Eur J Pediatr Surg, 2010. **20**(6): p. 363-5.

33. Moss, R.L., C.M. Chen, and M.R. Harrison, *Prosthetic patch durability in congenital diaphragmatic hernia: a long-term follow-up study.* J Pediatr Surg, 2001. **36**(1): p. 152-4.

34. Beres, A., et al., *Evaluation of Surgisis for patch repair of abdominal wall defects in children.* J Pediatr Surg, 2012. **47**(5): p. 917-9.

35. Romao, R.L., et al., *What is the best prosthetic material for patch repair of congenital diaphragmatic hernia? Comparison and meta-analysis of porcine small intestinal submucosa and polytetrafluoroethylene.* J Pediatr Surg, 2012. **47**(8): p. 1496-500.

36. Suply, E., et al., *Patch repair of congenital diaphragmatic hernia is not at risk of poor outcomes.* J Pediatr Surg, 2020. **55**(8): p. 1522-1527.

37. Russo, F.M., et al., *Current and future antenatal management of isolated congenital diaphragmatic hernia.* Semin Fetal Neonatal Med, 2017. **22**(6): p. 383-390.

38. Fauza, D.O., *Tissue engineering in congenital diaphragmatic hernia.* Semin Pediatr Surg, 2014. **23**(3): p. 135-40.

39. Badylak, S.F., D. Taylor, and K. Uygun, *Whole-organ tissue engineering: decellularization and recellularization of three-dimensional matrix scaffolds.* Annu Rev Biomed Eng, 2011. **13**: p. 27-53.

40. Crapo, P.M., T.W. Gilbert, and S.F. Badylak, *An overview of tissue and whole organ decellularization processes.* Biomaterials, 2011. **32**(12): p. 3233-43.

41. Maghsoudlou, P., et al., *Optimization of Liver Decellularization Maintains Extracellular Matrix Micro-Architecture and Composition Predisposing to Effective Cell Seeding.* PLoS One, 2016. **11**(5): p. e0155324.

42. Ott, H.C., et al., *Perfusion-decellularized matrix: using nature's platform to engineer a bioartificial heart.* Nat Med, 2008. **14**(2): p. 213-21.

43. Gerli, M.F.M., et al., *Perfusion decellularization of a human limb: A novel platform for composite tissue engineering and reconstructive surgery.* PLoS One, 2018. **13**(1): p. e0191497.

44. Soto-Gutierrez, A., et al., *A whole-organ regenerative medicine approach for liver replacement.* Tissue Eng Part C Methods, 2011. **17**(6): p. 677-86.

45. De Waele, J., et al., *3D culture of murine neural stem cells on decellularized mouse brain sections.* Biomaterials, 2015. **41**: p. 122-31.

46. Pati, F., et al., *Printing three-dimensional tissue analogues with decellularized extracellular matrix bioink.* Nat Commun, 2014. **5**: p. 3935.

47. Lee, H., et al., *Development of Liver Decellularized Extracellular Matrix Bioink for Three-Dimensional Cell Printing-Based Liver Tissue Engineering.* Biomacromolecules, 2017. **18**(4): p. 1229-1237.

48. Taylor, D.A., et al., *Decellularized matrices in regenerative medicine.* Acta Biomater, 2018. **74**: p. 74-89.

49. Sicari, B.M., et al., *An acellular biologic scaffold promotes skeletal muscle formation in mice and humans with volumetric muscle loss.* Sci Transl Med, 2014. **6**(234): p. 234ra58.

50. Qazi, T.H., et al., *Biomaterials based strategies for skeletal muscle tissue engineering: existing technologies and future trends.* Biomaterials, 2015. **53**: p. 502-21.

51. Kwee, B.J. and D.J. Mooney, *Biomaterials for skeletal muscle tissue engineering.* Curr Opin Biotechnol, 2017. **47**: p. 16-22.

52. Greising, S.M., et al., *Unwavering Pathobiology of Volumetric Muscle Loss Injury.* Sci Rep, 2017. **7**(1): p. 13179.

53. Fishman, J.M., et al., *Immunomodulatory effect of a decellularized skeletal muscle scaffold in a discordant xenotransplantation model.* Proc Natl Acad Sci U S A, 2013. **110**(35): p. 14360-5.

54. Valentin, J.E., et al., *Functional skeletal muscle formation with a biologic scaffold.* Biomaterials, 2010. **31**(29): p. 7475-84.

55. Gillies, A.R., et al., *Method for decellularizing skeletal muscle without detergents or proteolytic enzymes.* Tissue Eng Part C Methods, 2011. **17**(4): p. 383-9.

56. McClure, M.J., et al., *Decellularized Muscle Supports New Muscle Fibers and Improves Function Following Volumetric Injury.* Tissue Eng Part A, 2018. **24**(15-16): p. 1228-1241.

57. Urciuolo, A., et al., *Decellularised skeletal muscles allow functional muscle regeneration by promoting host cell migration.* Sci Rep, 2018. **8**(1): p. 8398.

58. Kasukonis, B., et al., *Codelivery of Infusion Decellularized Skeletal Muscle with Minced Muscle Autografts Improved Recovery from Volumetric Muscle Loss Injury in a Rat Model.* Tissue Eng Part A, 2016. **22**(19-20): p. 1151-1163.

59. Porzionato, A., et al., *Decellularized Human Skeletal Muscle as Biologic Scaffold for Reconstructive Surgery.* Int J Mol Sci, 2015. **16**(7): p. 14808-31.

60. Piccoli, M., et al., *Mouse Skeletal Muscle Decellularization.* Methods Mol Biol, 2018. **1577**: p. 87-93.

61. Urciuolo, A. and P. De Coppi, *Decellularized Tissue for Muscle Regeneration.* Int J Mol Sci, 2018. **19**(8).

62. Hussein, K.H., et al., *Biocompatibility evaluation of tissue-engineered decellularized scaffolds for biomedical application.* Mater Sci Eng C Mater Biol Appl, 2016. **67**: p. 766-778.

63. Wolf, M.T., et al., *Biologic scaffold composed of skeletal muscle extracellular matrix.* Biomaterials, 2012. **33**(10): p. 2916-25.

64. Bracey, D.N., et al., *A porcine xenograft-derived bone scaffold is a biocompatible bone graft substitute: An assessment of cytocompatibility and the alpha-Gal epitope.* Xenotransplantation, 2019. **26**(5): p. e12534.

65. Yang, Y.G. and M. Sykes, *Xenotransplantation: current status and a perspective on the future.* Nat Rev Immunol, 2007. **7**(7): p. 519-31.

66. Naso, F., et al., *First quantitative assay of alpha-Gal in soft tissues: presence and distribution of the epitope before and after cell removal from xenogeneic heart valves.* Acta Biomater, 2011. **7**(4): p. 1728-34.

67. Boso, D., et al., *Extracellular Matrix-Derived Hydrogels as Biomaterial for Different Skeletal Muscle Tissue Replacements.* Materials (Basel), 2020. **13**(11).

68. Engelmayr, G.C., Jr., et al., *A novel flex-stretch-flow bioreactor for the study of engineered heart valve tissue mechanobiology.* Ann Biomed Eng, 2008. **36**(5): p. 700-12.

69. Donnelly, K., et al., *A novel bioreactor for stimulating skeletal muscle in vitro.* Tissue Eng Part C Methods, 2010. **16**(4): p. 711-8.

70. Broer, T., A. Khodabukus, and N. Bursac, *Can we mimic skeletal muscles for novel drug discovery?* Expert Opin Drug Discov, 2020. **15**(6): p. 643-645.

71. Vandenburgh, H.H., *Mechanical forces and their second messengers in stimulating cell growth in vitro.* Am J Physiol, 1992. **262**(3 Pt 2): p. R350-5.

72. Kim, H., M.C. Kim, and H.H. Asada, *Extracellular matrix remodelling induced by alternating electrical and mechanical stimulations increases the contraction of engineered skeletal muscle tissues.* Sci Rep, 2019. **9**(1): p. 2732.

73. Moon du, G., et al., *Cyclic mechanical preconditioning improves engineered muscle contraction.* Tissue Eng Part A, 2008. **14**(4): p. 473-82.

74. Khodabukus, A. and K. Baar, *Glucose concentration and streptomycin alter in vitro muscle function and metabolism.* J Cell Physiol, 2015. **230**(6): p. 1226-34.

75. Khodabukus, A. and K. Baar, *Factors That Affect Tissue-Engineered Skeletal Muscle Function and Physiology.* Cells Tissues Organs, 2016. **202**(3-4): p. 159-168.

76. Langer, R. and J.P. Vacanti, *Tissue engineering.* Science, 1993. **260**(5110): p. 920-6.

77. McGreevy, J.W., et al., *Animal models of Duchenne muscular dystrophy: from basic mechanisms to gene therapy.* Dis Model Mech, 2015. **8**(3): p. 195-213.

78. Bartoli, M., et al., *Mannosidase I inhibition rescues the human alpha-sarcoglycan R77C recurrent mutation.* Hum Mol Genet, 2008. **17**(9): p. 1214-21.

79. Kobuke, K., et al., *A common disease-associated missense mutation in alpha-sarcoglycan fails to cause muscular dystrophy in mice.* Hum Mol Genet, 2008. **17**(9): p. 1201-13.

80. Caddeo, S., M. Boffito, and S. Sartori, *Tissue Engineering Approaches in the Design of Healthy and Pathological In Vitro Tissue Models.* Front Bioeng Biotechnol, 2017. **5**: p. 40.

81. Gentile, P., et al., *An overview of poly(lactic-co-glycolic) acid (PLGA)-based biomaterials for bone tissue engineering.* Int J Mol Sci, 2014. **15**(3): p. 3640-59.

82. Maffioletti, S.M., et al., *Three-Dimensional Human iPSC-Derived Artificial Skeletal Muscles Model Muscular Dystrophies and Enable Multilineage Tissue Engineering.* Cell Rep, 2018. **23**(3): p. 899-908.

83. Franzin, C., et al., *Isolation and Expansion of Muscle Precursor Cells from Human Skeletal Muscle Biopsies.* Methods Mol Biol, 2016. **1516**: p. 195-204.

84. Dumont, N.A., et al., *Satellite Cells and Skeletal Muscle Regeneration.* Compr Physiol, 2015. **5**(3): p. 1027-59.

85. Chen, W., D. Datzkiw, and M.A. Rudnicki, *Satellite cells in ageing: use it or lose it.* Open Biol, 2020. **10**(5): p. 200048.

86. Roca, I., et al., *Myogenic Precursors from iPS Cells for Skeletal Muscle Cell Replacement Therapy.* J Clin Med, 2015. **4**(2): p. 243-59.

87. Wang, J., et al., *Engineered skeletal muscles for disease modeling and drug discovery.* Biomaterials, 2019. **221**: p. 119416.

88. Piccoli, M., et al., *Improvement of diaphragmatic performance through orthotopic application of decellularized extracellular matrix patch.* Biomaterials, 2016. **74**: p. 245-55.

89. Urbani, L., et al., *Multi-stage bioengineering of a layered oesophagus with in vitro expanded muscle and epithelial adult progenitors.* Nat Commun, 2018. **9**(1): p. 4286.

90. Trevisan, C., et al., *Generation of a Functioning and Self-Renewing Diaphragmatic Muscle Construct.* Stem Cells Transl Med, 2019. **8**(8): p. 858-869.

91. de Cesare, N., et al., *A finite element analysis of diaphragmatic hernia repair on an animal model.* J Mech Behav Biomed Mater, 2018. **86**: p. 33-42.

92. Eshmuminov, D., et al., *Perfusion settings and additives in liver normothermic machine perfusion with red blood cells as oxygen carrier. A systematic review of human and porcine perfusion protocols.* Transpl Int, 2018.

93. Zhu, C.H., et al., *Cellular senescence in human myoblasts is overcome by human telomerase reverse transcriptase and cyclin-dependent kinase 4: consequences in aging muscle and therapeutic strategies for muscular dystrophies.* Aging Cell, 2007. **6**(4): p. 515-23.

94. Meran, L., et al., *Engineering transplantable jejunal mucosal grafts using patient-derived organoids from children with intestinal failure.* Nat Med, 2020.

95. Corona, B.T., et al., *The promotion of a functional fibrosis in skeletal muscle with volumetric muscle loss injury following the transplantation of muscle-ECM.* Biomaterials, 2013. **34**(13): p. 3324-35.

96. Fanning, K.M., et al., *Changes in microvascular density differentiate metabolic health outcomes in monkeys with prior radiation exposure and subsequent skeletal muscle ECM remodeling.* 2017. **313**(3): p. R290-R297.

97. Osses, N. and E. Brandan, *ECM is required for skeletal muscle differentiation independently of muscle regulatory factor expression.* 2002. **282**(2): p. C383-94.

98. Petrosino, J.M., A. Leask, and F. Accornero, *Genetic manipulation of CCN2/CTGF unveils cell-specific ECM-remodeling effects in injured skeletal muscle.* FASEB J, 2019. **33**(2): p. 2047-2057.

99. Lee, H., et al., *A novel decellularized skeletal muscle-derived ECM scaffolding system for in situ muscle regeneration.* Methods, 2020. **171**: p. 77-85.

100. Alabi, B.R., R. LaRanger, and J.W. Shay, *Decellularized mice colons as models to study the contribution of the extracellular matrix to cell behavior and colon cancer progression.* Acta Biomater, 2019. **100**: p. 213-222.

101. Chen, H.J., et al., *A recellularized human colon model identifies cancer driver genes.* Nat Biotechnol, 2016. **34**(8): p. 845-51.

102. Piccoli, M., et al., *Decellularized colorectal cancer matrix as bioactive microenvironment for in vitro 3D cancer research.* J Cell Physiol, 2018. **233**(8): p. 5937-5948.

103. D'Angelo, E., et al., *Patient-Derived Scaffolds of Colorectal Cancer Metastases as an Organotypic 3D Model of the Liver Metastatic Microenvironment.* Cancers (Basel), 2020. **12**(2).

104. Sensi, F., et al., *Recellularized Colorectal Cancer Patient-derived Scaffolds as in vitro Pre-clinical 3D Model for Drug Screening.* Cancers (Basel), 2020. **12**(3).

105. Powell, C.A., et al., *Mechanical stimulation improves tissue-engineered human skeletal muscle.* 2002. **283**(5): p. C1557-65.

106. Vandenburgh, H.H., *Motion into mass: how does tension stimulate muscle growth?* Med Sci Sports Exerc, 1987. **19**(5 Suppl): p. S142-9.

107. Vandenburgh, H.H., et al., *Skeletal muscle growth is stimulated by intermittent stretch-relaxation in tissue culture.* Am J Physiol, 1989. **256**(3 Pt 1): p. C674-82.

108. Vandenburgh, H.H. and P. Karlisch, *Longitudinal growth of skeletal myotubes in vitro in a new horizontal mechanical cell stimulator.* In Vitro Cell Dev Biol, 1989. **25**(7): p. 607-16.

109. Vandenburgh, H.H., et al., *Mechanically induced alterations in cultured skeletal muscle growth.* J Biomech, 1991. **24 Suppl 1**: p. 91-9.

110. Walker, M., et al., *Structural and mechanical remodeling of the cytoskeleton maintains tensional homeostasis in 3D microtissues under acute dynamic stretch.* Sci Rep, 2020. **10**(1): p. 7696.

111. Anloague, A., et al., *Mechanical stimulation of human dermal fibroblasts regulates pro-inflammatory cytokines: potential insight into soft tissue manual therapies.* BMC Res Notes, 2020. **13**(1): p. 400.

112. Zein-Hammoud, M. and P.R. Standley, *Modeled Osteopathic Manipulative Treatments: A Review of Their in Vitro Effects on Fibroblast Tissue Preparations.* J Am Osteopath Assoc, 2015. **115**(8): p. 490-502.

113. Trevisan, C., et al., *Allogenic tissue-specific decellularized scaffolds promote long-term muscle innervation and functional recovery in a surgical diaphragmatic hernia model.* Acta Biomater, 2019. **89**: p. 115-125.